Polymeric Microfluidic Platforms for Immunodetection

Dissertation presented

By

Vincent LINDER

Institute of Microtechnology, University of Neuchâtel, Switzerland

In collaboration with:

Department of Clinical Pharmacology, University of Bern, Switzerland

Centre Suisse d'Electronique et de Microtechnique SA, Switzerland

IMPRIMATUR POUR LA THESE

Polymeric Microfluidic Plattform for Immunodetection

de M. Vincent Linder

UNIVERSITE DE NEUCHATEL

FACULTE DES SCIENCES

La Faculté des sciences de l'Université de Neuchâtel sur le rapport des membres du jury,

Mme E. Verpoorte,
MM. N. de Rooij (directeur de thèse), R. Tabacchi,
H. Sigrist (CSEM, Neuchâtel) et J. Harrison
(Edmonton Canada)

autorise l'impression de la présente thèse.

Neuchâtel, le 15 février 2002

Le doyen:

F. Zwahlen

Table of contents

Introduction

PLATFORMS FOR MICROFLUIDICS

Pioneering work from H. Michael Widmer's group in the early 90's was aimed at the miniaturization of analytical systems in order to establish fast and sensitive methods (1). The first application reported was the implementation of capillary electrophoresis (CE) separations on planar glass chips (2). CE in its conventional form is performed in a one-dimensional fused silica capillary, and requires the introduction of a large amount of sample into the capillary (c.a. 1% of the total length, 1-50 nL) in order to achieve reproducible separations. The use of two-dimensional microfluidic channel networks enables the handling of much smaller sample volumes. The time required for the separation of individual species from a sample decreases with sample volume. With microfluidic systems, it is possible to achieve the delivery of pL sample volumes, and therefore, CE-on-chip can be performed considerably faster than regular CE. Optimization of channel geometry and electric fields in a chip enabled sub-millisecond separation time (3). As foreseen by Widmer and Manz, the application of bi-dimensional integrated systems goes far beyond the scope of fast CE separations. The design of interconnected channels and reaction chambers of various sizes could ultimately yield a chip that can process a sample through all the steps usually carried out in a laboratory. This concept is known as the Minaturized Total Analysis System (μTAS) or Lab-on-a-chip. Numerous sample-handling steps have been individually realized on microfluidic platforms, such as serial/parallel dilutions (4), pneumatic mixing (5), organic synthesis (6), PCR (7) and cell handling (8). Recent developments are well covered in reviews (9, 10). The coupling of sample-handling steps on a single chip will provide μTAS chips with fully automated preparation and fast analysis of samples. The use of miniaturized systems will also require less power and smaller amounts of reagent to perform the assays. Since most of the analytical steps of the assay take place on the chip, the instruments that run the μTAS chip will be small, highly automated and possibly portable.

Several techniques developed for the microelectronics industry have been directly used for the fabrication of microfluidic platforms. For instance, photolithographic processes based

on photosensitive polymers give access to patterned surfaces. Selective etching of the patterned materials enables micromachining of the surface to obtain microchannels. Moreover, selective metal deposition can be used for the fabrication of microelectrodes for the purpose of electrochemical detection or dielectrophoresis. The first materials investigated were Pyrex (2) and quartz (11) (SiO_2) because they were chemically inert, transparent, and therefore suitable for fluorescence measurements. Another widely used material is silicon, which can be easily micromachined using the numerous techniques available from the microelectronics industry. However, silicon is not transparent, is unstable in the presence of alkaline solutions, and cannot withstand the high voltages required to move liquids electroosmotically (12). Therefore, silicon has been found more attractive as a substrate for microchannel replication in polymers (see later) than as a material for microchip fabrication. In these materials, three different channel cross sections are available (see Figure 1). Two etching methods taking place in aqueous media are available. KOH-wet etching on silicon provides trapezoidal profiles, whereas HF-wet etching of SiO_2 gives rectangular profiles, with rounded sidewalls. These techniques are well suited for low height/width aspect ratios. In a dry environment, rectangular structures of high aspect ratio can be obtained by deep reactive ion etching (DRIE).

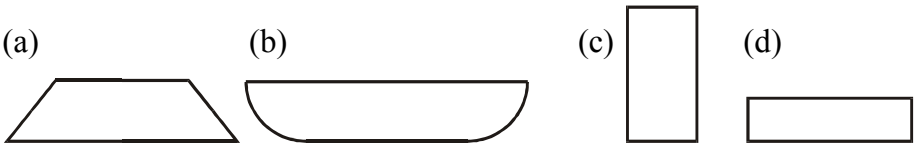

Figure 1: Several types etching profile are obtained by varying the etching conditions. (a) KOH-wet etching of silicon, (b) HF-wet etching in SiO_2 substrates and (c, d) DRIE.

Due to the high costs of microfabrication technology and the starting material described above, polymeric materials have been used for the mass production of batches of structures at low costs. However, polymeric microchannels are generally more hydrophobic and don't have electrical charges on their surface, resulting in stronger sample adsorption to channel walls and lower electroosmotic flows (EOF, see later the discussion about EOF) (17). Poly(dimethylsiloxane) (PDMS) has been reported as an attractive material for microchannel replication (13-15). Structured PDMS surfaces are obtained quickly and are transparent over the entire visible spectrum of light. Moreover, PDMS replicates can be sealed to virtually any flat material to obtain channels. The use of other polymers such as

acrylic copolymer (16-17), poly(methylmethacrylate) (PMMA) (18), polystyrene (PS) (17), copolyester (17) and poly(ethyleneterephtalate) glycol, (PETG) (19) have also been reported. These microfluidic platforms are obtained by replication of a master pattern into polymeric materials, using casting, hot embossing or injection molding techniques. Fabrication of the original master pattern requires a high level of precision and is often carried out in a clean room environment by silicon etching, thick photoresist patterning (with e.g. SU-8) or growth of galvanic structures. Casting is the quickest method to set up and is appropriate for the fabrication of small series of prototypes. Hot embossing enables the fabrication of hundreds or thousands of prototypes, but requires more complicated instrumentation for the tight control of temperature and applied pressure during the embossing step. Injection molding (20) is carried out only in an industrial environment for the mass production of inexpensive replicated chips, and is certainly not appropriate for prototyping.

MASS TRANSPORT TECHNIQUES IN MICROCHANNELS

Glass materials are made of SiO_2, with SiOH groups at the surface. These groups behave like weak acids and therefore remain protonated (SiOH form) in acidic media, but dissociate when pH is gradually increased to reach alkaline conditions. The pK_a value of SiOH groups is approximately 6 (21). Thus in neutral or alkaline aqueous conditions, the surface of channels made of SiO_2 material (fused silica, quartz, Pyrex or glass) is covered by fixed, negatively charged SiO^- groups that are counterbalanced by a layer of cations (often Na^+). Upon application of an electric field along the channel, all electric charges will experience a dragging force towards the electrode of opposite sign. The layer of positively charged counter ions will move towards the cathode, dragging solvent with them. However, the negatively charged SiO^- groups are bound to the surface by covalent bonds, and therefore cannot be displaced in the electric field.

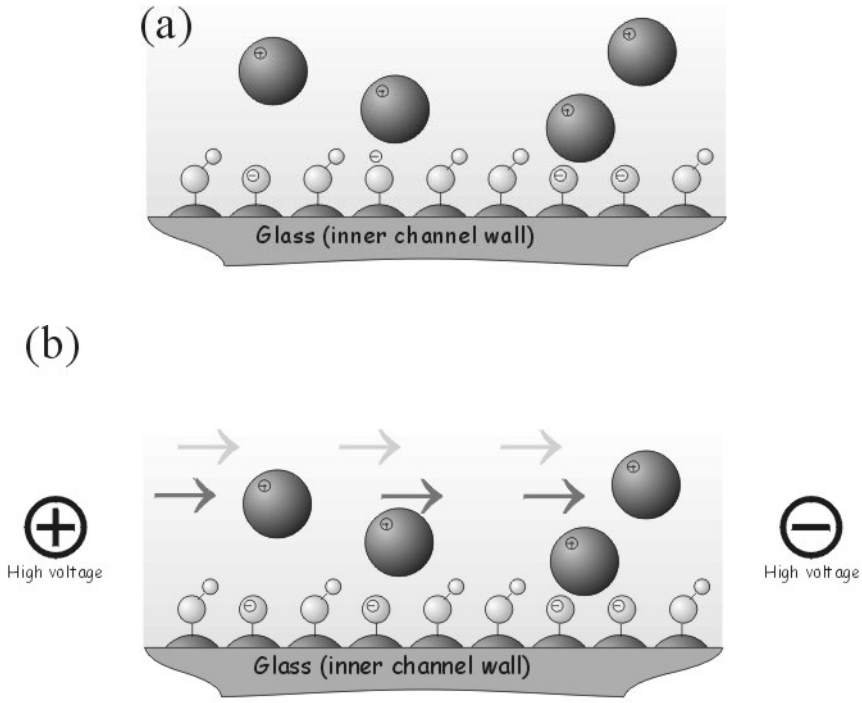

Figure 2: Schematic view of electroosmotic flow generation. (a) In a neutral or alkaline pH, the negatively charged SiO^- groups are electrically counterbalanced by a diffuse layer of cations. (b) Upon application of a high electric field, the motion of the cations is transferred to the rest of the liquid.

Thus, a net mass flow towards the cathode is observed in a thin annular region close to the surface. This motion is transferred to the rest of the liquid contained in the capillary by viscous forces and is refered to as electroosmosis (see Figure 2). The transfer process to the fluid located at the channel center takes less than 1 ms. This phenomenon is strongly dependent on the presence of electrically charged groups at the surface of the material, and the more groups, the stronger the electroosmosis. A physical unit known as zeta potential (ζ), describes the difference in potential close to the surface. The solution present at the interface is capable of changing ζ, either by increasing the number of electric charges at the material surface (e.g. using a more alkaline buffer) or by changing the distance between the wall and the plane of shear, where ζ is defined (e.g. varying the buffer ionic strength). The viscosity-induced motion transfer mechanism from the surface to the bulk liquid is also influenced by variation in temperature (22). The resulting electroosmotic mass transport velocity (v_{EOF}) is described by the equation 1:

$$v_{EOF} = \mu_{EOF} \cdot E \qquad \text{with} \qquad \mu_{EOF} = \frac{\varepsilon \cdot \zeta}{\eta} \qquad [1]$$

Where μ_{EOF} is the electroosmotic mobility, ε is the dielectric constant, ζ is the zeta potential and η is the solution viscosity. Unfortunately, electroosmosis cannot be used in electrically conductive substrates, due to its requirements for high voltages. Therefore, silicon microstructures, though easily processed, cannot withstand the voltages required for electroosmosis (12), whereas SiO_2 channels are fully suitable.

Mass transport in the microfluidic network is also possible using pressure-driven flows (either positive or negative pressure). In theory, pressure-driven flows do not downscale well, since smaller channel dimensions require a higher pressure drop in order to maintain the flow velocity. However, they are easily set up and are suitable for mass transport in channels made of conductive material, such as silicon. The major difference between electroosmotic and pressure-driven flow lies in the velocity profile in the channel. In case of pressure-driven flows, the flow velocity is zero at the channel wall, and gradually increases towards the center of the channel, according to a parabolic profile. Therefore, a section of fluid introduced into a channel will be distorted upon transport, as the fluid located in the central part of the channel moves faster than that close to the walls (see Figure 3a).

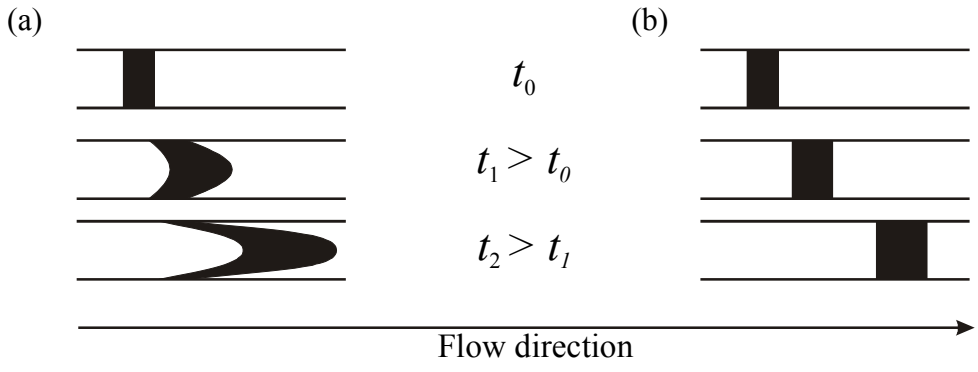

Figure 3: (a) Sample zone distortion vs. time is large for pressure-driven flow systems, due to the high transport velocity in the center of the channel compared to the rest of the channel. (b) In case of electroosmosis, sample zone broadening is mostly governed by diffusion. Other effects arising from electromigration are also possible.

However, electroosmotic transport is characterized by a uniform distribution of flow velocities over the channel (see Figure 3b), except very close to the channel walls. For liquid chromatography applications, the separations appear more efficient using electroosmosis than pressure-driven flows, due to lower dispersion by the flow profile. When manipulating flows in complex microchannel networks, electroosmotic pumping is a convenient tool for tuning liquid flow in individual channels, by varying the applied voltages at each channel end. However, upon application of a high electric field in a microchannel, electrophoresis takes place as well. Therefore the apparent transport velocity is the sum of the electroosmotic and electrophoretic velocities. In channels made of glass (SiO_2 in general), and under alkaline conditions, electroosmosis is strong and overrules electrophoresis, resulting in a net flow of most analytes in the direction of the cathode. However, the cations will be displaced faster than the electroosmotic flow, whereas the anions will be retarded. Electroosmotic flow velocity is characterized by the parameter μ_{EOF}, which is specific for each material and liquid. The electroosmotic mobility of a material is commonly measured using either a current monitoring method (23) or by recording the migration time of a neutral marker. The use of an electrically neutral molecule is important, in order to eliminate the electrophoretic contribution to the transport.

FLUORESCENCE

Most molecules have the ability to absorb photons at a given wavelength, and during this process the photon transfers its energy to the molecule. This excess energy is normally dissipated in the form of vibration, rotation or translation. However, some molecules have the ability to re-emit part of this energy as longer wavelength photons, by means of fluorescence. In more detail, upon absorption of a photon, an electron gains enough energy to move from a ground state energy towards an excited state. The electron will then lose part of its energy by internal conversion to reach the lowest energy mode of the excited state. Finally, the electron returns to the ground state energy, and the remaining energy is released in the form of a photon. Due to the loss of energy during the internal conversion in the excited state, the total energy of the emitted photon is lower than that of the excitation photon. The resulting difference between the excitation and emission wavelength is called the Stokes' shift. The presence of a small shift in wavelength enables the detection of a small number of emitted photons in presence of large excess of excitation photons. A

molecule can repeat a fluorescence emission cycle numerous times (e.g. fluorescein, 30'000 cycles), before the excited state alters the molecular structure. Therefore, upon long exposure time or high light intensities, the fluorescence signal decreases proportionally to the excitation light intensity, a phenomenon known as photobleaching.

Many chemical structures are known to be fluorescent, one of the most common being fluorescein (see Figure 4a). The spectral characteristics of the fluorescing base structures are sensitive to their chemical environment. One example is fluorescein, which is excited at 488 nm. Addition of four electron-rich bromine atoms and a sulfonic group on the π-system (see Figure 4b) modifies the electronic environment and shifts the excitation to 532 nm. Cyanine dyes are composed of heterocyclic ends linked by a variable spacer arm. The length of the spacer determines the spectral characteristics of the dye. For instance, the 5C-atom long spacer of Cy5 (Figure 4c) makes for an excitation wavelength of 650 nm, whereas a 3-atom long spacer shifts the excitation down to 532 nm (Cy3).

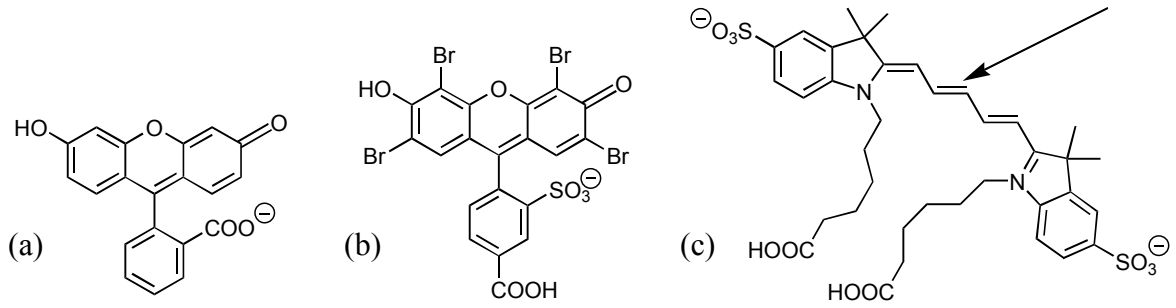

Figure 4: Chemical structure of selected examples of fluorescent dyes. (a) Fluorescein, (b) 2',4',5',7'-tetrabromosulfone fluorescein and (c) Cy5. The arrow indicates the 5-atom long spacer.

Generally, the fluorescent molecule structure requires the mobility of a free electron in a large system of alternating double bonds or heteroatoms. The carboxylic group of fluorescein is therefore not well suited for observation in acidic media. However, cyanine dye contains negatively charged sulfonic groups, which remain deprotonated in acidic media. The structural modification of known fluorescent molecules has made available numerous dyes of varying properties (e.g. solubility in aqueous buffers, pH-insensitive fluorescence, enhanced stability against photobleaching or large Stockes' shift). Multi-dye

observation is also possible, using a series of dyes in which the excitation and emission wavelengths do not overlap.

ANTIBODY STRUCTURE AND CHEMISTRY

Antibodies, also called immunoglobulins, are proteins produced by the immune system for the defense of the organism against foreign species. They consist mainly of amino acids but also contain varying amounts of carbohydrate residues (3-12%), whose biological role is not well understood. Immunoglobulins are made of two heavy and two light chains of amino acids, forming a characteristic Y-shape. Disulfide bridges hold the heavy chains together to form the Y, whereas each light chain is bound to a branch of the Y to obtain the final structure (see Figure 5). The extremities of the Y branches have a well-defined 3-dimensional shape, which is designed to specifically bind a target, or antigen, by a lock-and-key mechanism. Potentially harmful foreign species (the keys) are therefore recognized by the immunoglobulins (locks) in the presence of numerous other molecules, and subsequently deactivated upon formation of a very stable immunocomplex. The very high antigen specificity of immunoglobulin is achieved thanks to a complex 3-dimensional arrangement of the amino acids, where a perfect match is obtained. The shape, the polarity and the electric charges of the key have to fit precisely into the lock (see expanded view in Figure 5). The stability of the overall antibody structure relies on a cooperative effect of numerous weak interactions between side chains of amino acids in the protein backbone.

The sum of all weak interactions gives a strong structure. However, perturbation of a few weak interactions upon changes in pH or ionic strength, or chemical modification, may result in important changes in the tertiary shape of the immunoglobulin, and perhaps the loss of its affinity for a target.

Each target requires a different recognition structure, and therefore a great variability is observed at the ends of the arms of a set of immunoglobulins. However, the rest of the protein shows little variation. Thus, immunoglobulin structure is split into two regions, one of variable composition, the other of constant composition (see *a* and *b* in Figure 5). Immunoglobulins are classified into five classes (IgG, IgA, IgM, IgD and IgE) on the basis of the composition of their constant region. For a given animal, all immunoglobulins of a given class have essentially the same constant region, which is slightly different from those of another class. However, interspecies variations are observed for immunoglobulins, e.g. a

goat may produce a *goat anti-mouse IgG*, which specifically binds any IgGs of a mouse, without interacting with IgGs from other animals.

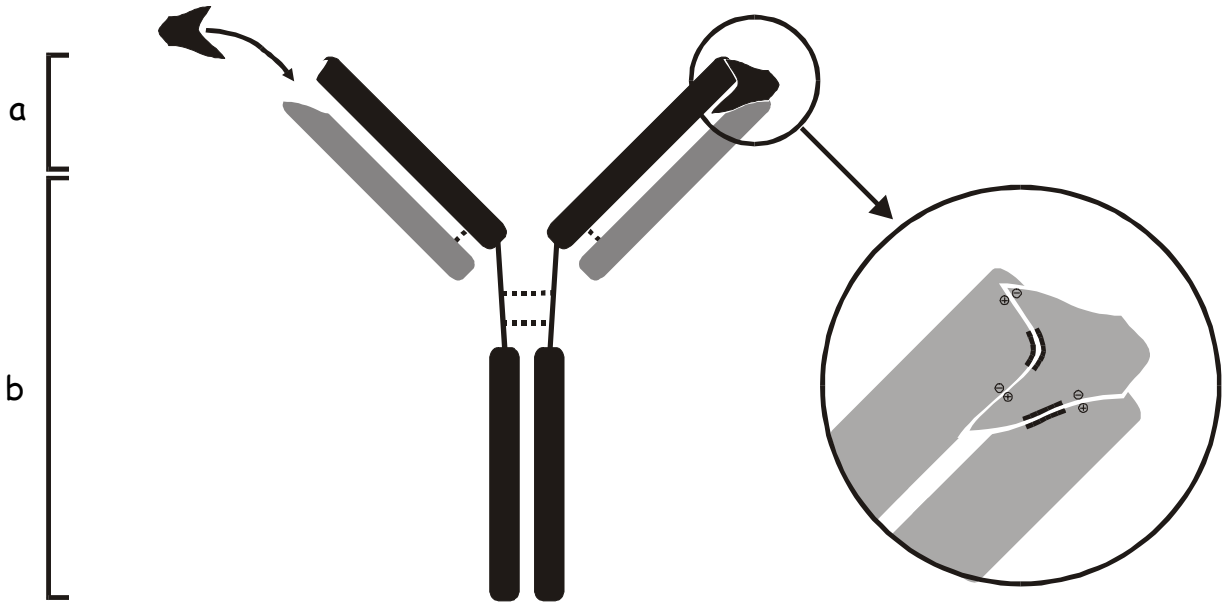

Figure 5: Schematic structure of an immunoglobulin protein. Two heavy chains (black) are linked by disulfide bridges (dotted lines) in the central part, which is known as the Hinge region. The bottom part of the protein (all black) is known as F_c region. Light chains (grey) are bound to the heavy chains by other disulfide bridges. Letters *a* and *b* indicate the variable and constant regions, respectively. The tips of the variable regions exhibit a specific tertiary structure, in which an antigen strongly interacts (see arrow). The expanded view shows in more detail how the antigen fits into the antibody. Electrical charges of the antigen (+/-) are locally counterbalanced by the protein, and hydrophobic domains (black lines) of the antigen and antibody also match well.

A wide choice of commercially available specific antibodies can be purchased for qualitative and/or quantitative assays. Most antibodies are used to trace specific targets in tissues, liquids or surfaces. Whatever the assay conditions, the final stage requires antibody or antigen detection. For that purpose, antibodies are labeled prior to the assay by molecules characterized by their fluorescence, radioactivity, enzymatic activity, chemiluminescence or mass. Specific reagents have been developed to attach to proteins at almost any position. By far the most common coupling reactions take place with amino

groups. However, other chemically reactive groups, such as thiols, carboxylates, hydroxyls or carbonyls, may also be used as an anchor. Amine modification relies on the coupling reaction between an amino group of the protein with the activated group of a label. Chemical activation of the label is essential to obtain a sufficient amount of label on the protein. Historically, labeling with isothiocyanate-activated groups has been extensively used, for instance with fluorescein isothiocyanate, resulting in the formation of a stable thiourea bond (Figure 6a). More recently, N-hydroxysuccinimide- (NHS-) activated labels have become commercially available. NHS activation of a carboxylic group on the label yields very reactive species towards amines, producing an amide linkage (e.g. NHS-Cy5 in Figure 6b). Owing to their higher reactivity towards amines, labeling with NHS-activated molecules takes place 10 to 50 times faster than using the more traditional isothiocyanate chemistry.

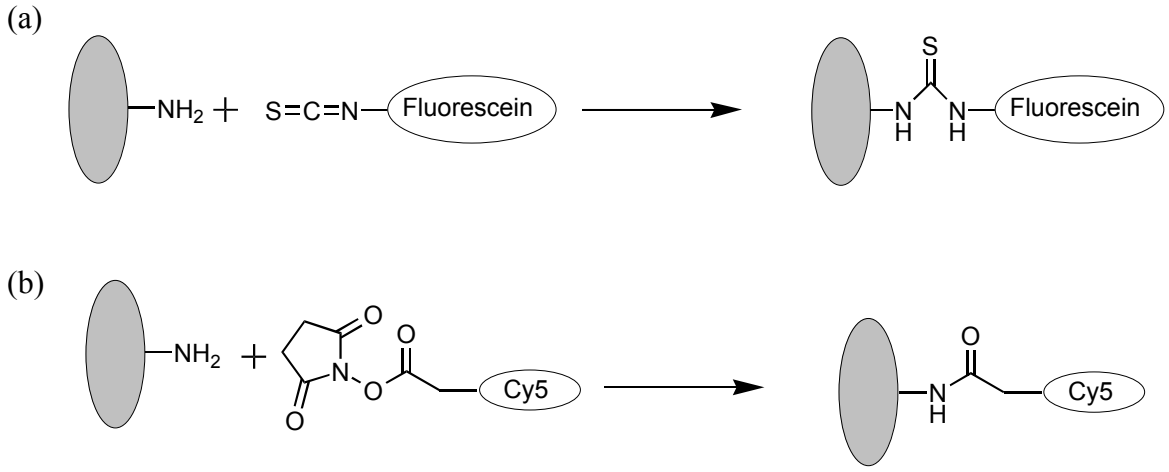

Figure 6: Two examples of activated fluorescent molecules designed for coupling with an amino group of a protein (represented by a gray ellipse, not to scale). (a) Fluorescein isothiocyanate undergoes a coupling reaction to form a thiourea link, whereas (b) NHS-Cy5 is coupled upon formation of an amide bond.

A protein contains numerous free amino groups. Some of them are buried in the protein bulk and hold the overall structure together by participating in stabilizing interactions with other amino acids, whereas others are pointing out of the bulk and are therefore easily accessible. Coupling of several labels on a single IgG first takes place on the accessible amino groups. However, forcing the coupling of numerous labels may result in the

modification of an amino group involved in a stabilizing interaction, and consequently in the modification of its chemical environment. For instance, the linkage of a Cy5 fluorescent molecule, via NHS-Cy5 (see Figure 6b) modifies a small positively charged amino group into a bulky hydrophobic derivative that contains a negative charge. Under such an enormous change in chemical environment, the amino group loses its stabilizing interactions, and the tertiary structure of the protein is locally altered. The result of such a coupling reaction near the binding site of the antibody is the loss of its recognition ability. It is therefore important to tune the amount of label to insure sensitive detection, without destroying the antibody affinity for a target.

During the coupling reaction between an antibody and an excess of amino-reactive activated label, most of the reagent is hydrolyzed by the OH^- groups contained in water. Therefore, unbound label has to be removed from the antibody-containing solution either by exclusion chromatography or by immunoprecipitation. Exclusion chromatography is a separation technique relying on the use of a sugar-based gel that contains a controlled distribution of pores. Upon migration of a multi-component sample through the gel by gravitationally induced flow, small molecules have a chance to enter the pores and thus escape from the flow. Therefore, large molecules travel faster than small ones, and the sample components are separated by size. In the case of antibody labeling, the antibody is typically 150 times larger than the label, and fast separations are carried out easily. Separation by immunoprecipitation is based on the specific binding of IgG by protein A- or protein G-coated beads. The binding takes place at the IgG F_c region (see Figure 5), and the species-related small variations in that region are responsible for the varying affinity constants between protein A or G and IgGs. After incubation of the antibody-containing solution with the protein-coated beads, all IgGs are affinity-bound to the solid support. Undesired chemicals are washed away by centrifugation and IgGs are released by breaking the affinity bonds under acidic conditions, where the protein structures are altered due to an increased net charge.

IMMUNOASSAYS

The use of antibodies for clinical assays was first reported in the 1960's, with a competitive radioimmunoassay for insulin (24). Over the last 40 years, much progress in assay design has been achieved. Long-term efforts have been devoted to the replacement of radioactive

tracers by various fluorescent, chemiluminescent or enzyme labeled-tracers, yielding similar or better assay sensitivity (24). The first significant improvement was the development of antibody labeling and its application to "two-site" immunoassay (sandwich), where two antibodies bind an antigen at two different sites, a basic requirement for non-competitive immunoassays (see below). Later, the bioengineering of monoclonal antibody enhanced the sensitivity and the specificity of immunoassays.

Immunoassays were first designed with a competitive format, with the non-competitive approach being developed later. In a competitive or "limited reagent" method, a limited number of antibodies are incubated with a sample containing a mixture of antigen and labeled antigen. Both species will compete for the few binding sites available on the antibodies. The antigen/labeled antigen ratio bound to the antibodies (or left out due to insufficient number of binding sites) is proportional to the initial ratio in the sample (see Figure 7). Hence, knowing the initial amount of labeled antigen added and determining the ratio of labeled to unlabeled antigen measured by competitive immunoassay, the original antigen concentration can be deduced.

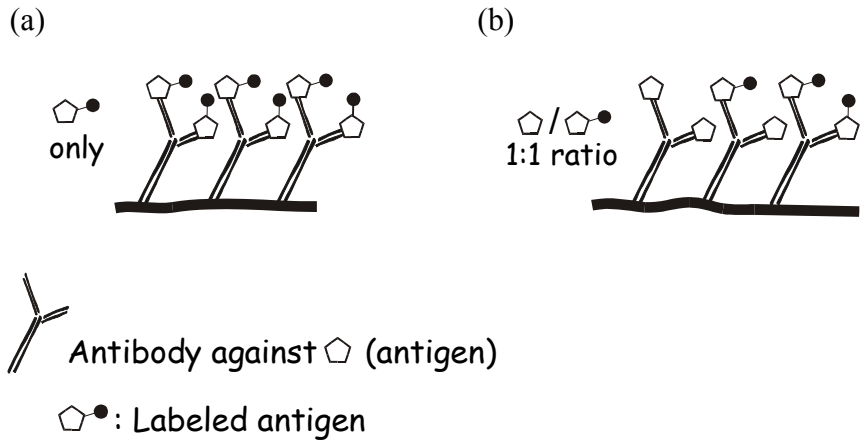

Figure 7: In a competitive immunoassay, the bound species reflect the ratio of antigen to labeled antigen in solution. (a) A sample containing only labeled antigen gives rise to a large label signal, whereas (b) in presence of a 1:1 ratio of labeled to unlabeled antigen in sample, the label signal drops by half. (This assumes that labeled and unlabeled species bind at the same rates. However, slight differences or loss of affinity may occur upon labeling.)

Competitive immunoassays are easily set up, but suffer from several disadvantages, including: (i) a limited sensitivity and working range, (ii) slow reaction kinetics, (iii) increased imprecision and (iv) the development of negative end-points. Negative end-points are characterized by very low fluorescence signals for samples of high antigen content, which could be also caused by a faulty assay (e.g. due to pipetting or dilution error, use of degraded reagents or wrong automatic sample addressing).

These disadvantages have been overcome by the introduction of a non-competitive immunoassay format, using a sandwich immunoassay and labeled antibodies. This assay format requires the use of two sets of antibodies, each one being able to recognize the antigen structure at a different location. Antigens from a dilute sample are concentrated upon binding to an excess of specific antibodies immobilized on a solid support. The affinity bond between the antigen and the primary antibody occurs at one antigen location. Then, a secondary labeled antibody is reacted with the bound antigen by affinity binding at another antigen location. The label signal that is measured is directly proportional to the amount of antigen pre-concentrated on the primary antibody.

The final quantitative result from an immunoassay is obtained by recording the signal produced by the labeled partners (antigen or antibody) of the immunoreaction. Quantification is possible by recording either the free or the bound labeled partner, but these species first have to be physico-chemically separated. In homogeneous immunoassays, all partners are in solution, and the physico-chemical separation is often carried out by gel or capillary electrophoresis. Alternatively, the fluorescence produced by the bound species can be optically isolated by fluorescence polarization. However, immobilization of an immunoreaction probe on a solid substrate (e.g. wells, microtubes or beads) prior to running the assay forces the reaction to take place on the support and later reduces the separation step to a simple support washing, precipitation, or bead centrifugation. Moreover, the use of a heterogeneous format enables the preconcentration of the species in solution onto the solid support and therefore enhances the sensitivity of the assay. However, the uncontrolled adsorption of the solute onto the solid support surface can yield a significant background signal, which dramatically reduces the assay sensitivity (see Figure 8). Therefore, all heterogeneous immunoassays require the use of an efficient surface chemistry, which eliminates non-specific binding (NSB). The most popular approaches rely on the physisorption of bovine serum albumin or the use of diluted sample.

Surface chemistry can also help achieve better overall orientation of the antibodies for more efficient binding and enhanced affinity.

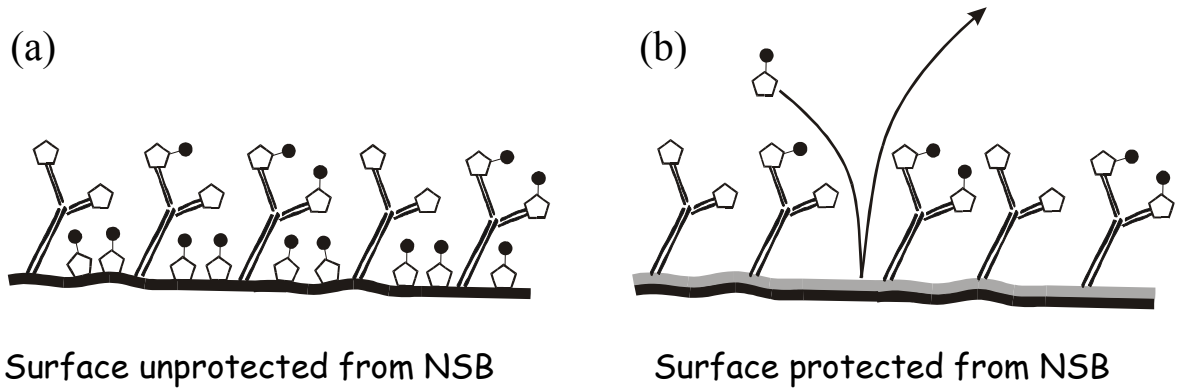

Figure 8: (a) In the absence of a NSB-eliminating surface chemistry, antigen adsorption to the solid support surface during the immunoassay can result in a very large background signal. (b) However, the use of an appropriate surface treatment (grey layer) eliminates adsorption, and all benefits from a solid phase assay are obtained.

Goals of the work

The overall goal of this work was to develop a single-use microfluidic device for the immunological detection of clinically relevant species, such as human IgG. Poly(dimethylsiloxane) (PDMS) was chosen as a material for channel fabrication because of its optical transparency, ease of use and possible modification with a stable physisorption-based coating. Electrokinetically driven sample transport was used for its ease of tuning individual fluid flow velocities in the channel network. Moreover, electrokinetic effects are responsible for transporting analyte and tracer at different velocities.

For the purpose of developing an electrokinetically driven assay in a PDMS/glass microfluidic platform, electroosmosis in microchannels was studied. Several physico-chemical treatments of the PDMS surface prior to sealing on glass were considered. The hydrophobic PDMS surface was shown to suffer from severe adsorption, and therefore the deposition of a passivating surface coating was investigated. Integration of biotinylated probes was possible in the outer layer of the three-layer biotin/neutravidin-based sandwich coating. Selective deposition of biotinylated anti-human IgG in the microfluidic platform was developed using a laminar flow-based patterning technique. The feasibility of a heterogeneous immunoreaction between anti-human IgG immobilized in the channels and Cy5-labeled human IgG in an electrokinetically transported liquid sample was demonstrated. Qualitative monitoring of the bound Cy5-human IgG was achieved by fluorescence microscopy. Quantitative measurements with a fluorescence scanner originally designed for arrays required changes in the chip design. Reproducibility and confidence in the assay results were enhanced by the implementation of an internal standard. This was done by co-immobilizing biotinylated anti-mouse IgG along with anti-human IgG in the biospecific region of the chip. A competitive immunoassay for human IgG was set up, using Cy5-human IgG as bound tracer and Cy3-mouse IgG as internal standard. The ratio of Cy5 to Cy3 signal was used to assess the original human IgG concentration, while absence of Cy3 signal was indicative of faulty chip function. Human IgG concentration dependence was investigated under physiological and alkaline

conditions. Finally, monitoring of serum human IgG levels of patients and its potential application to diagnostics was investigated.

Most of the work done in this project has been presented in two articles. Therefore, the early results that are not covered by the articles will be presented in detail and a short summary of the published work will follow. For more details, the articles have been attached in their original form in the appendices.

Experimental section

This section describes the methodologies that were used to conduct the experiments carried out during the first part of this project, which was not submitted for publication. Methodologies utilized in the rest of the work are included in the publications, copies of which are attached in this dissertation as appendices.

MICROFLUIDIC DESIGN WITH STRAIGHT CHANNELS

The channel layout depicted in Figure 9a was realized in a chromium mask (Delta Mask, Enschede, Netherlands). The design contained straight channels of varying width (10, 30, and 50 μm) and a longer, 30 μm wide channel laid out in a serpentine manner. In this particular design, current monitoring measurements could be performed in channels of varying width and length (4, 6.5 and 37.8 cm).

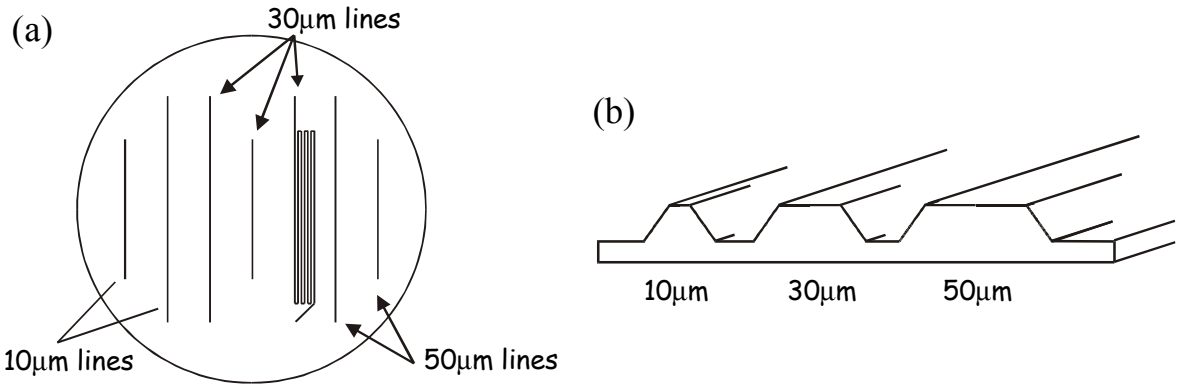

Figure 9: (a) The design of the master used for PDMS channel microfabrication contains several straight channels of varying length and width. (b) Channel profile obtained after KOH wet etching for each channel width.

PDMS MICROFLUIDIC PLATFORM PREPARATION

Silicon wafer micromachining provided masters for polymer replication of the layouts presented in Figure 9a. After photolithography and photoresist development, the silicon

was KOH-wet-etched to obtain 19-µm-deep structures (see Figure 9b). Residual photoresist was dissolved in acetone, and rinsed off with isopropanol. Before replication, the silicon surface was treated with octadecyldimethylchlorosilane, and fixed in a specially designed holder. Dow Corning PDMS Sylgard 184 obtained from Distrelec (Nänikon, Switzerland) was prepared according to the manufacturer's directions, by mixing 1 part catalyst with 10 parts base resin. The pre-polymer was poured onto the master and cured at 65°C for 4 h. The finished PDMS slab was peeled off and 4-mm-diameter access holes to the channels were punched out using a cork borer. The replica was cleaned by ultrasonic treatment in isopropanol, followed by water (5 min each).

PDMS was prepared in several forms, referred to as native, aged or plasma-oxidized, and then sealed to a Pyrex substrate to form a hybrid device refered to as PDMS/Pyrex system. The native PDMS channels were obtained by using replicas produced as described above without further treatment. Aging of PDMS relied on a 12-hour thermal treatment at 115°C, followed by ultrasonic cleaning in isopropanol and water (see details above). Channels were formed by sealing the PDMS replica onto an unstructured AF45 glass wafer (Schott, Feldbach, Switzerland)). Prior to sealing, the glass substrate was degreased in hexane (5 min), treated in aqueous HCl 5% (5 min) to render the surface hydrophilic, and rinsed in water. Glass and PDMS substrates were dried under vacuum ($5 \cdot 10^{-2}$ mbar) for 1 h. Reversible sealing of PDMS on glass was realized without further treatment. Plasma-oxidized channels were obtained upon plasma oxidation of both substrates prior to sealing. RF-induced 100 W oxygen plasma treatment was carried out for 15 s in a Plasmalab 80plus (Oxford Instruments, Bristol, UK) in 0.3 mbar O_2. Channels were filled with 50 mM phosphate buffer (PBS; pH 7.4, containing 150 mM NaCl) until use. Prior to the first measurements, filtered (0.45µm), 0.1 M NaOH solution was flushed into the channels, and allowed to interact with the PDMS for about 90 minutes. Finally, the system was conditioned again in PBS and stored at RT.

CURRENT MONITORING IN CHANNELS

A complete set of measurements consisted of two types of experiments. First, the sealing quality and the cleanliness of the microchannels (absence of clogs) were assessed by establishing a current response curve at varying applied voltages. Channels and reservoirs were filled with a fresh 20 mM sodium phosphate buffer (pH 7.0), and the current was

measured at increasing voltages ranging from 0V to 8000V. After every 800 V increase, the system was allowed to stabilize for 10 s, before recording the current. If measured currents agreed with calculated values for the channel geometry and solution conductivity in question, good sealing and clear channels were assured. The electroosmotic mobility was then measured in the channels using a method based on current monitoring (23). Channels were flushed with a fresh 20 mM buffer. One reservoir was then filled with slightly diluted, 19 mM buffer, and 20 mM buffer was introduced into the opposite reservoir. Hydrostatic pressure-driven flows were avoided by filling the reservoirs to equal levels. Electroosmotic flow was then generated in such a way that the dilute buffer entered the channel. As this buffer replaced the 20 mM buffer, current flowing through the channel was recorded and filtered using a digital low-pass filter operating at 30 Hz. After current signal stabilization, reservoirs were conditioned with fresh buffers and the reverse experiment was carried out. The electroosmotic flow velocity could then be calculated for both experiments by dividing channel length by the time required for the current to reach a stable value, at which point all buffer solution in the channel had been replaced. Electroosmotic flow velocity measurements were repeated using varying electric fields.

Results and discussion

In this section, the results obtained during the first part of the project are presented in detail and their implications for the following work are discussed. Then, the key points for the rest of the work are summarized. More information about this latter part of the work is available in the appendices of the dissertation.

PART I: ELECTROOSMOTIC MOBILITY IN PDMS CHANNEL

When electroosmotic mobility is determined by current monitoring, a slightly diluted buffer enters the channel and replaces the same buffer at its original concentration. The concentrations of the buffer used should vary by no more than 5 %, to ensure that the assumption of a constant ζ potential is valid. As the buffer of lower ionic concentration enters the channel, the current flowing through the channel decreases gradually until the diluted buffer reaches the channel end (see Figure 10). Afterwards, the current becomes stable again.

The electroosmotic flow velocity is calculated by dividing the time required to reach a steady current by the length of the channel. The electroosmotic mobility is then calculated using Equation 2, where v_{eo} is the electroosmotic flow velocity, μ_{eo} the electroosmotic mobility (see Equation 1) and E the electric field.

$$v_{eo} = \mu_{eo} \cdot E \qquad [2]$$

Electroosmotic velocities were measured for several electric fields ranging from 300 to 1100Vcm^{-1}, and plotted versus the applied electric field to obtain a straight line. The slope of the line, which is the electroosmotic mobility, was obtained by linear regression.

Day-to-day reproducibility of the electroosmotic mobility was investigated in native PDMS/glass devices with 20 mM phosphate buffer (pH 7.0). Intermittent measurements were carried out over a period of 38 days, with the channels stored filled with PBS buffer between measurements. Electroosmotic mobility was shown to decrease by 6 % over this period (see Figure 11a), with an initial value of $4.46 \cdot 10^{-4}$ cm^{2}V^{-1}s^{-1}. The variations in electroosmotic mobility between a series of native PDMS/Pyrex devices were shown to be

less than 10 % (see Figure 11b). The average electroosmotic mobility was found to be $4.99 \cdot 10^{-4}$ $cm^2V^{-1}s^{-1}$.

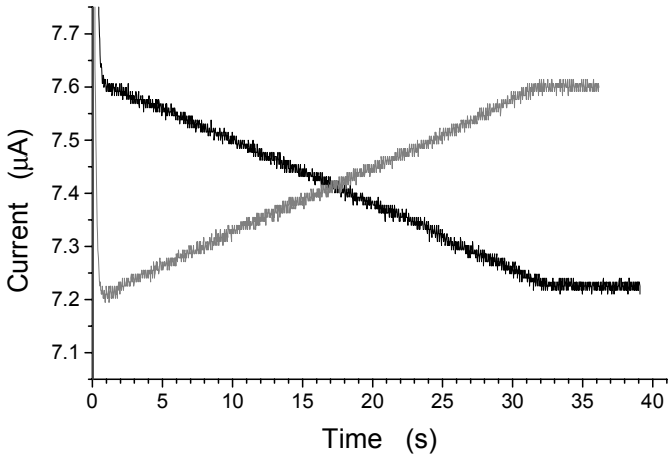

Figure 10: Electroosmotic velocity determination by current monitoring relies on the introduction of a more dilute buffer into a channel (black solid line). The experiment can also be conducted in reverse, to monitor the introduction of a more concentrated buffer into a channel (grey solid line). Experimental conditions: 19 and 20 mM phosphate buffer in a 30 µm wide PDMS/glass channel, under an electric field of 500 Vcm^{-1}.

The influence of surface treatment on the electroosmotic mobility was also investigated for a single, freshly prepared PDMS replica. Electroosmotic mobility was measured in the PDMS/glass device before and after thermal aging and after plasma oxidation. Electroosmotic mobility determination took place directly after surface treatment. Variations in electroosmotic mobilities were less than 10 % (see Figure 12). Plasma-oxidized PDMS appeared more hydrophilic than the native or aged elastomer. Despite that, aging and plasma treatment of PDMS had no significant effect on EOF, other than to improve the precision of the measurements. Linear regression calculations to obtain the electroosmotic mobility also yielded an associated error value, which was highest for the native PDMS/glass channel (see Table 1). The observed electroosmotic mobility in PDMS/glass channels is the sum of contributions from both materials. Therefore, the unchanged glass surface may partially mask the changes accuring on the PDMS surface. Changes in PDMS surface may be investigated in a 100% PDMS channel.

(a)

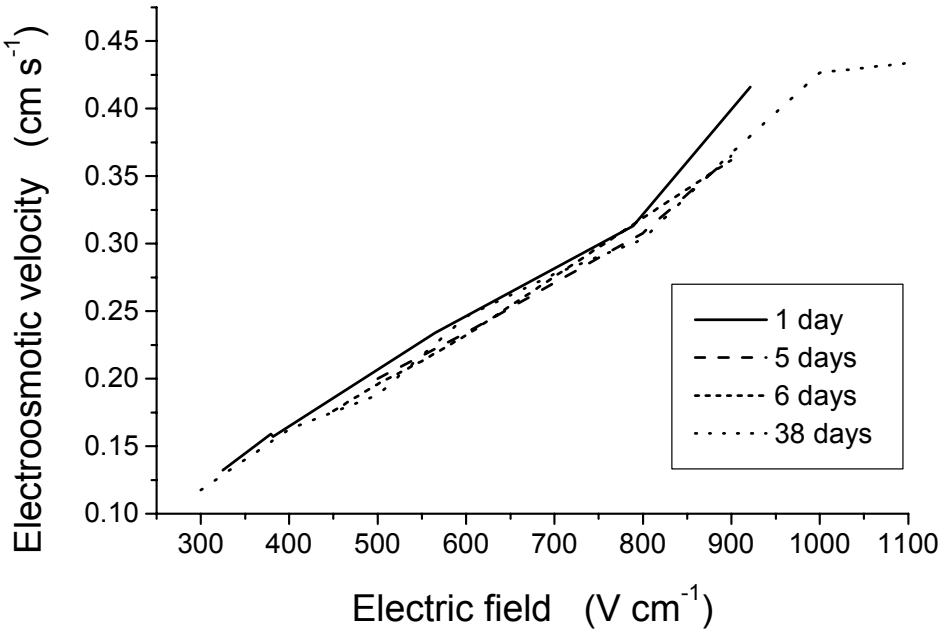

(b)

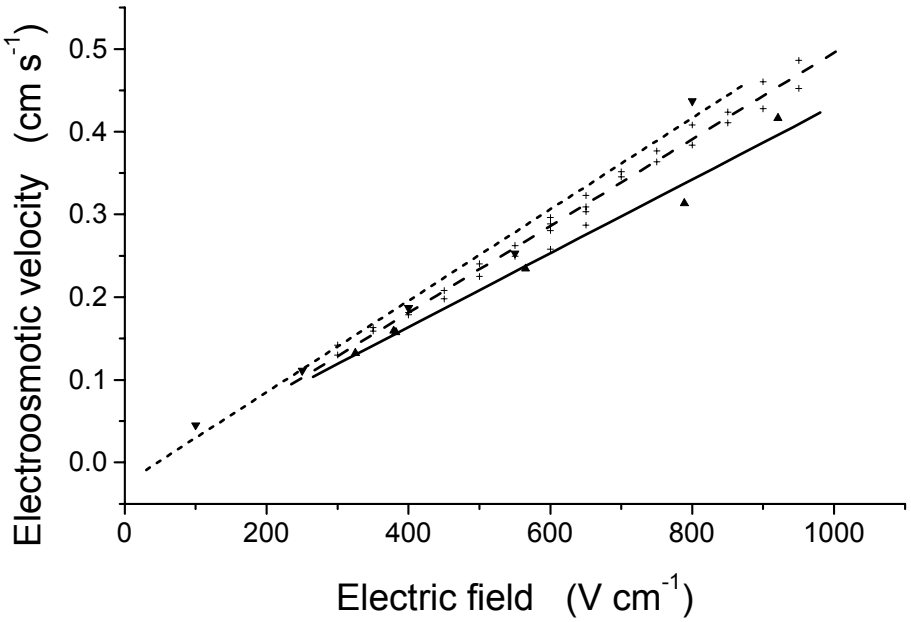

Figure 11: (a) Electroosmotic mobility monitoring in a single native PDMS/glass device over a 38-day time period. All data were obtained using the same channel. (b) Variations in electroosmotic mobility between three freshly prepared native PDMS/glass devices, #1 (triangles, line: solid), #2 (crosses, line: long dash) and #3 (downwards pointing triangles, line: short dash). Data points for each device were obtained using channels of various cross-sections (30, 50, 70 μm lines, see Figure 9) available on the device. Straight lines were calculated by linear regression.

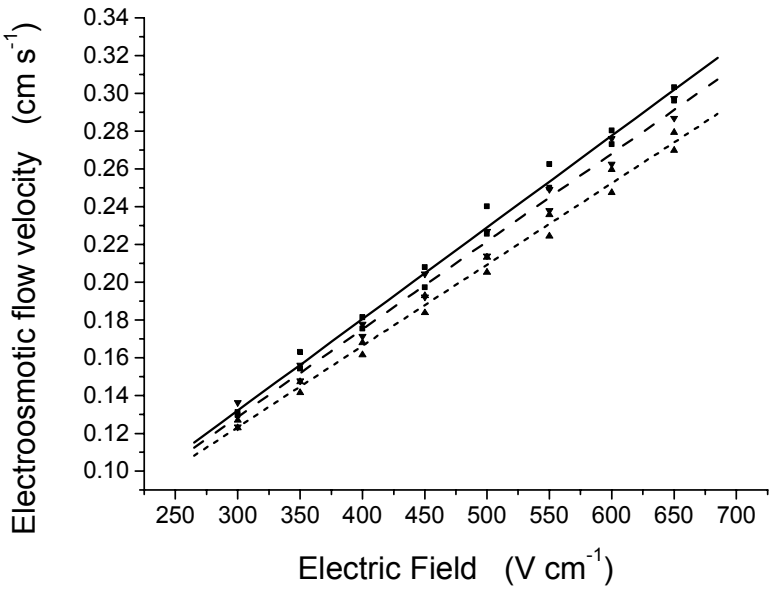

Figure 12: Electroosmotic flow velocity monitoring in a single PDMS/glass channel in a native form (squares, line: solid), after thermal aging (downward pointing triangles, line: long dash) and after plasma oxidation (upward pointing triangles, line: short dash). Electroosmotic mobility determination took place directly after surface treatments. Data points for each device were obtained using channels of various cross-sections (30, 50, 70 μm lines, see Figure 9) available on the device. Straight lines were calculated by linear regression.

Table 1: Calculated electroosmotic mobilities as a function of the surface treatment. Values, errors and correlation coefficients were all calculated by linear regression.

Device	Measurements	Electroosmotic mobility ($cm^2V^{-1}s^{-1}$)	Std. Dev. on mobility ($cm^2V^{-1}s^{-1}$)	Correlation coefficient (linear regression)
Standard	16	$4.85 \cdot 10^{-4}$	$1.50 \cdot 10^{-5}$	0.996
Aged	16	$4.31 \cdot 10^{-4}$	$5.13 \cdot 10^{-6}$	0.9995
Plasma-treated	16	$4.65 \cdot 10^{-4}$	$7.07 \cdot 10^{-6}$	0.9994

According to optical microscope observation, the thinner channels (10 μm) replicated into PDMS were occasionally damaged upon separation from the master. However, high replication quality was achieved for the 30 μm and 50 μm channels, as well as good EOF reproducibility according to current monitoring. Due to the large cross section of the 50 μm channels, large currents were observed, giving rise to Joules heating effects at relatively low electric fields. Therefore, the optimal channel size was found to be about 30 μm.

Applications for diagnostic microfluidic chips require reproducible channel surfaces, which remain unchanged over extended period of time. Surface treatment such as thermal aging or plasma treatment appeared to have a minor influence on the electroosmotic mobility intensity. However, current monitoring measurements were shown to be more reproducible in aged and plasma-treated channels than in native channels. The monitoring of a neutral fluorescent marker in thermally aged channels showed that the hydrophobic PDMS surface suffered from severe adsorption problems. In plasma-treated channels, adsorption problems appeared to be eliminated, but the adsorptive properties of the oxidized surface changed dramatically within 9 h (see Appendix 1 for more details). As a result of these preliminary experiments, the use of thermally aged PDMS appeared preferable to native PDMS, due to its higher EOF reproducibility and long-term stability. The plasma oxidation approach was discarded, due to the resulting surface instability.

The main conclusion drawn from these initial studies was that an appropriate surface treatment for thermally aged PDMS microfluidic platform had to be established, both to eliminate the adsorptive properties of the hydrophobic surface, and to make possible the analysis of hydrophobic samples in the channels. This led to the development of the three-layer, biotin-neutravidin-based biopassivation coating, TERACOAT, described in the next section, and in Appendix 1.

PART II: DEVELOPMENT OF A PLATFORM FOR IMMUNOREACTION

This part presents a summary of the work that aimed at development of a platform for immunoreaction. The original article is provided in Appendix I (or Linder V., Verpoorte E., Thormann W., de Rooij N.F., Sigrist H. *Anal. Chem.*, **2001**, 73, 4181-4189.).

PDMS surface modification – TERACOAT

Handling of biological samples in PDMS/glass channels using electrokinetic sample transport was the starting point of this project. To that end, electroosmotic mobility was investigated by the current monitoring method and by neutral fluorescent marker displacement. The neutral dye, tetramethylrhodamine-dextran, was successfully used for electroosmotic mobility determination in Pyrex channels. However, when applied to PDMS/glass channels, tetramethylrhodamine-dextran appeared to adsorb to the elastomer surface. Further experiments showed that many constituents of biological fluids, such as proteins, were adsorbing onto the elastomeric surface as well. Thus, the deposition on PDMS of a coating made of three successive layers of biopolymers was investigated. The strong adsorptive properties of PDMS were exploited for the physisorption of biotin-conjugated goat anti-mouse IgG. Neutravidin was then linked to biotin by affinity interaction, producing a second layer. Neutravidin is a bioengineered derivative of avidin that is neutral under physiological conditions, and was used instead of streptavidin or avidin to avoid possible interactions with charged molecules in solution. Finally, a layer of biotin-conjugated dextran was bound to unoccupied biotin-binding sites of the tetravalent neutravidin. The overall surface treatment was called TERACOAT (referring to TERnary Affinity COATing), see Figure 13a. Surface modification considerably decreased adsorption of low and high molecular mass substances to channel walls, while maintaining a modest cathodic electroosmotic flow. A surface passivation based on IgG physisorption was investigated because IgGs have a strong hydrophobic interaction with materials such as PDMS. And the use of biopolymers as blocking agent was found to be efficient to prevent adsorption of other biopolymers on the treated surface.

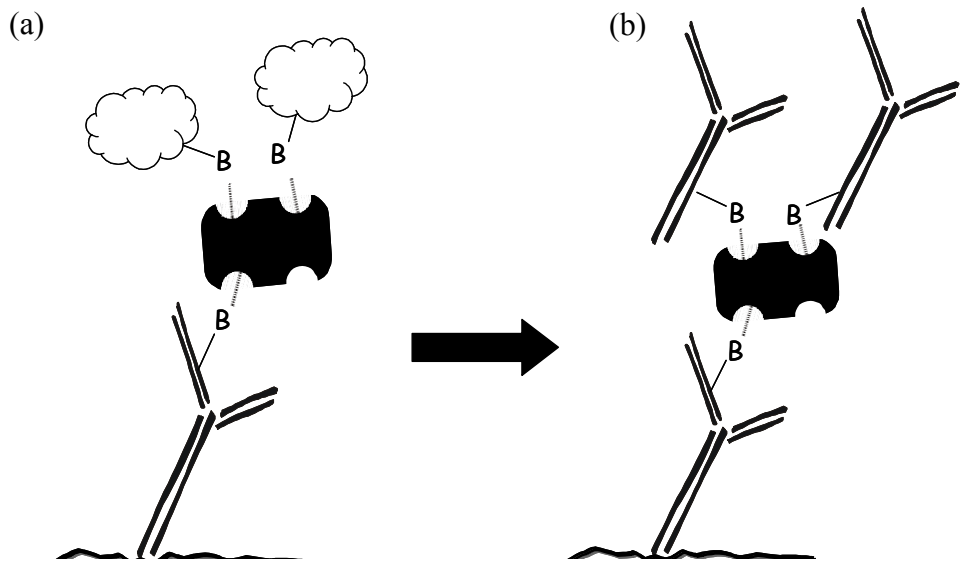

Figure 13: Schematic diagram of (a) TERACOAT and (b) TERASYS. The first IgG layer was physisorbed to the PDMS, whereas the second and third layers were fixed using highly specific biotin-neutravidin binding. In the third layer the channel was patterned with either biotinylated dextran (TERACOAT) or biotinylated antibody (TERASYS).

Coating stability in various liquids was studied by fluorescence microscopy using a TERACOAT containing fluorescein-labeled neutravidin. Desorption was monitored by recording the loss of fluorescence in the coating. TERACOAT was shown to be stable for one hour exposure to water, 7.92 mM phosphate buffer (pH 7.0) and 6.74 mM tetraborate buffer (pH 9.3). All solutions were continuously drawn through the channel using vacuum. Moreover, no degradation was observed when biological matrices such as serum or human urine were applied. However, the coating was slowly damaged by weak detergents. After one hour exposure to Tween 20® (0.02% (v/v) in 7.92 mM phosphate buffer, pH 7.0) and 1 min rinsing with 7.92 mM phosphate buffer (pH 7.0), fluorescence was reduced by approximately 50%. TERACOAT desorption was observed in the presence of sodium dodecylsulfate (SDS, 10 mM in 6.74 mM tetraborate buffer, pH 9.3), or 0.1 M NaOH. After one hour of exposure and 1 min rinsing with 7.92 mM phosphate buffer (pH 7.0), the fluorescence due to the TERACOAT could not be distinguished from background.

The long-term stability of TERACOAT in 6.74 mM tetraborate buffer (pH 9.3) was investigated by CZE over one month. Chips were stored filled in running buffer at room temperature. Detection times of tetramethylrhodamine dextran were shown to decrease about two-fold, the largest drop being observed during the first hundred hours. RSD values of detection times for each set of 10 measurements were found to be less than 2 %, indicating that operation of the chip was reproducible on the hour time scale. For all these experiments, the shape of the tetramethylrhodamine-dextran peak did not change. Thus, the favorable passivation properties of TERACOAT appeared to be stable under CZE conditions over longer periods of time.

On-chip heterogeneous immunoreaction - TERASYS

A variation of TERACOAT deposition enabled the selective deposition of antibodies at specific locations in the channel network. This surface preparation was named TERASYS (referring to TERnary Affinity SYStem). The first layer (biotin-conjugated goat anti-mouse IgG) and second layer (neutravidin) were deposited as described above for TERACOAT. In the third layer, the channel network was partially coated with biotinylated goat anti-mouse antibodies to be used later for the immunoassay, and the remaining area was coated with inert biotin-conjugated dextran, see Figure 13b. The spatial resolution of the immobilized biomolecules was achieved using a flow patterning technique. Reservoirs 1 and 3 (numbering according to Figure 14a) were filled with a solution of biotin-conjugated dextran, and a solution of biotinylated goat anti-mouse IgG was pipetted into reservoir 4. Suction pumping at reservoir 2 generated three converging laminar flows towards vacuum. Biotinylated species attached to the neutravidin surface according to the flow profiles. Thus, a strip of antibodies was immobilized between reservoirs 4 and 2, while side channels were covered with dextran (as shown in Figure 14a).

Immunoreaction between immobilized goat anti-human IgG and Cy5-human IgG was investigated. A solution of Cy5-human IgG (200 μg/mL (1.33 μM) in PBS) was electrokinetically transported from reservoir 1 to 3 (see Figure 14b). It is interesting to note that, under the chosen conditions, Cy5-human IgG is negatively charged and migrates in the direction opposite to EOF. Incubation under electrokinetic conditions was carried out for 6 min, and the sensing area was subsequently rinsed with running buffer for 1 min (see

Figure 14c). Three important pieces of information can be extracted from the sensing area imaged by the fluorescence scanner (Figure 15a).

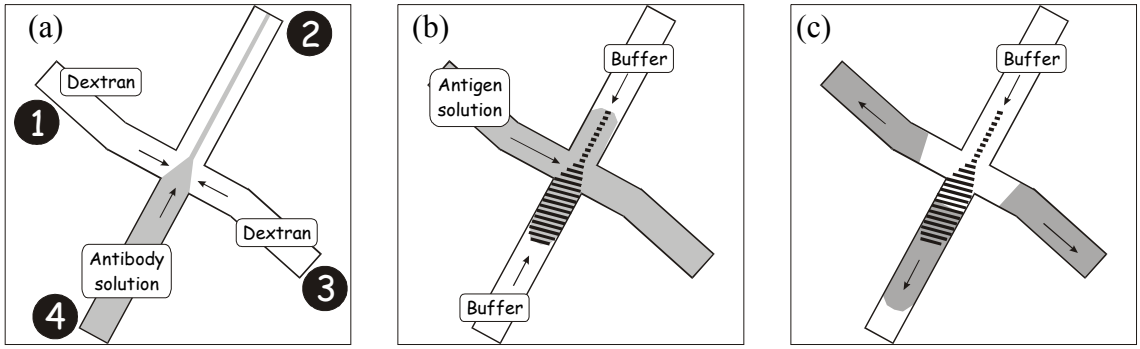

Figure 14: Schematic representation of the flow patterns applied for an on-chip immunoreaction. (a) Bio-probe patterning: the biotin-conjugated goat anti-human IgG was immobilized on the neutravidin-coated surface. The immobilization pattern followed the laminar flow profiles generated by vacuum pumping at reservoir 2. (b) Immuno-reaction takes place at the intersection where antibodies are immobilized and in contact with sample (hatched area). Cy5-human IgG (antigen) was electrokinetically delivered across the antibody-coated intersection. Side buffer flows were kept much smaller than sample flow, such that no flow patterning was observed at the cross. (c) Unbound antigen was removed by electrokinetic pumping without removing the bound antigen (hatched area).

First, the binding of Cy5-human IgG to the immuno-probe can be quantified. Secondly, light detected in the bottom left channel reveals the system background value (such as scattered light at material interfaces, for instance). Thirdly, non-specific binding (NSB) of Cy5-human IgG to the coated surface can be extracted from the top left channel or bottom right channel. The extent of analyte specific binding is obtained by subtracting the NSB value from the measured signal, and sample compatibility with TERACOAT is quantified by the difference between the background value and NSB.

Eight disposable TERASYS chips were tested, and signal intensity appeared to be reproducible (Figure 15b). An average signal value of 18380 RFU was obtained, associated with a chip-to-chip RSD of 18 %. Background values reached 40 RFU, whereas fluorescence related to Cy5-human IgG NSB was 89 RFU, about twice the background

value. Hence, the system was found to be fully adequate for a Cy5-human IgG immunoreaction.

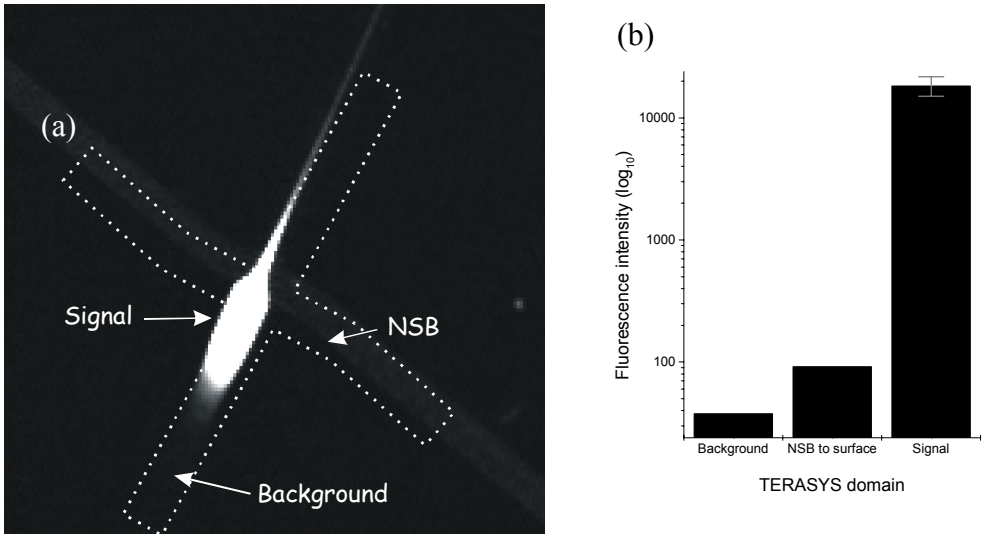

Figure 15: (a) Bound antigen image at the cross area obtained with the fluorescence scanner. Signal is observed at the intersection where the biotin-conjugated goat anti-human IgG pattern is immobilized and immunostained with Cy5-human IgG. Information on background levels and non-specific binding (NSB) can be extracted from the same experiment (b) Plot of average fluorescence intensities recorded in 8 TERASYS chips (log scale).

PART III: IMMUNOASSAY FOR HUMAN IgG

This part presents a summary of the work that involved the implementation of an internal standard on the chip, and the development of an immunoassay for human IgG. The original article, is available in Appendix II (or Linder V., Verpoorte E., de Rooij N.F., Sigrist H., Thormann W. *Electrophoresis*, **2002**, in press).

Incorporation of an internal standard into the TERASYS platform

The TERASYS platform characterized earlier was further developed for the analysis of human IgG in serum by a competitive immunoassay. A potential clinical application of the TERASYS chips requires an enhanced reproducibility for the immunoreaction (e.g. much less than 18 %) and a high level of confidence in the results obtained. TERASYS chips described in this contribution are single-use disposable devices that cannot be calibrated or tested prior to use. Therefore, an internal standard was implemented in the TERASYS chips, by immobilizing biotinylated goat anti-mouse IgG and biotinylated goat anti-human IgG in equal amounts in the sensing area. Samples containing 665 nM Cy3-mouse IgG and 665 nM mixtures of Cy5-human IgG/human IgG (different ratios) were then reacted in the chips. Recording fluorescence using 532 and 635 nm laser lines provided individual measurements for Cy3 and Cy5. An abnormally low or missing Cy3 signal indicated that TERASYS was not working, while minor chip-to-chip variations were compensated for by using the Cy5/Cy3 signal ratio.

On-chip competitive immunoassay for human IgG

Competition in the human IgG immunoassay took place in TERASYS chips, but assay sensitivity had a strong dependence on the running buffer pH. Electrokinetic transport of sample was very different in physiological buffer (pH 7.4) than under alkaline conditions (pH 9.3). Unlabeled and fluorescently labeled IgGs were observed to migrate very slowly in a direction opposite to electroosmotic flow at pH 7.4. However, at pH 9.3, the observed migration was with the electroosmotic flow. Typical net mobilities of Cy3-mouse IgG were about $6.5 \cdot 10^{-5}$ $cm^2 s^{-1} V^{-1}$ towards the cathode at pH 9.3 and towards the anode at pH 7.4.

Fluorescent labeling of IgG introduced additional negative charges to the IgG molecules. Therefore, when migrating against the EOF at pH 7.4, Cy5-human IgG reached the intersection first and could react initially with immobilized antibodies without competition. Competitive immunoassay therefore takes place only with the remaining free binding sites, resulting in poor assay sensitivity. However, at pH 9.3, both labeled and unlabeled human IgG migrated with EOF, with the less negatively charged unlabeled species arriving first at the intersection. Hence, initial human IgG binding took place under non-competitive conditions, yielding enhanced assay sensitivity, as shown in Figure 16.

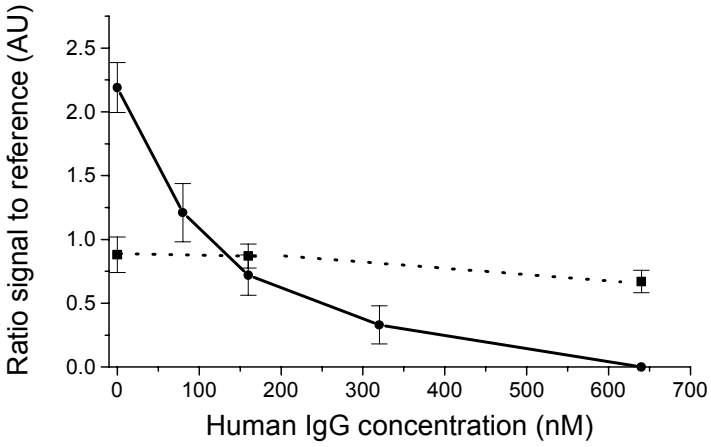

Figure 16: Calibration curve for human IgG competitive immunoassay. Sensitivity was enhanced when changing pH from 7.4 (dotted line) to 9.3 (solid line), which resulted in arrival of unlabeled antigen at the intersection prior to labeled antigen, leading to increased binding of the former species.

The immunoassay of the synthetic preparation of human IgG under alkaline conditions enabled detection down to 50 nM (7.5 µg/mL), with 6.8 % RSD (a value calculated by averaging RSD from 4 sets of data, n_{tot} = 17). The incubation time (not optimized) was set to 7 min to insure saturation of all binding sites on the surface. The heterogeneous format of the assay may enable the analysis of more dilute samples by allowing longer incubation times.

The long-term stability of fully prepared TERASYS chips was investigated using two means of chip storage, (i) at 4°C in PBS and (ii) at –20°C after buffer vacuum evaporation.

After a two-month storage period, immunoassays using a 1:1 Cy3-mouse IgG/Cy5-human IgG solution were performed under alkaline running conditions. Data obtained in chips stored at 4°C compared well with measurements made in fresh TERASYS chips. However, in the reconstituted dry-stored chips, the surface passivation was not active anymore, and an immunoassay could not be carried out**.**

IgG monitoring in human serum

Analysis of human serum failed when using the same experimental conditions as for the data presented in Figure 16. However, determination of IgG in human serum was shown to be possible using a different sample preparation. The four sera obtained from the clinical chemistry laboratory of the Inselspital (Berne, Switzerland) were then prepared with a larger excess of tracer (final human IgG concentration were 5.11, 8.50, 19.72 and 35.94 nM). Each sample was analyzed on four, freshly prepared, TERASYS chips. From the 16 runs, the data of 6 chips were discarded after weak internal standard signals indicated a faulty chip. Results obtained in the properly working TERASYS chips showed a concentration dependence for human IgG (Figure 17). A plot of the data obtained with synthetic and serum samples on the same scale showed that the dynamic range for determination of human IgG concentration in real samples was substantially smaller than for synthetic samples. Further work is required to properly elucidate the reasons for this pronounced sensitivity to sample matrix effects. Two phenomena are likely to be responsible: (i) an interfering species contained in serum sample may affect the antigen binding in TERASYS, or (ii) the absorption of serum component on the coating may affect the electrokinetic mechanism of sample delivery, and hence, assay sentivity.

The exact quantification of human IgG in serum was found to be difficult, due to the high RSD at a low human IgG concentration and the low concentration sensitivity at higher IgG levels. However, the data obtained for the two patients with normal IgG levels can be clearly distinguished from the data of the two other patients, who had elevated IgG levels caused by a chronic infection and cancer myeloma, respectively. The limit of detection for human IgG in serum samples was estimated at about 5 nM.

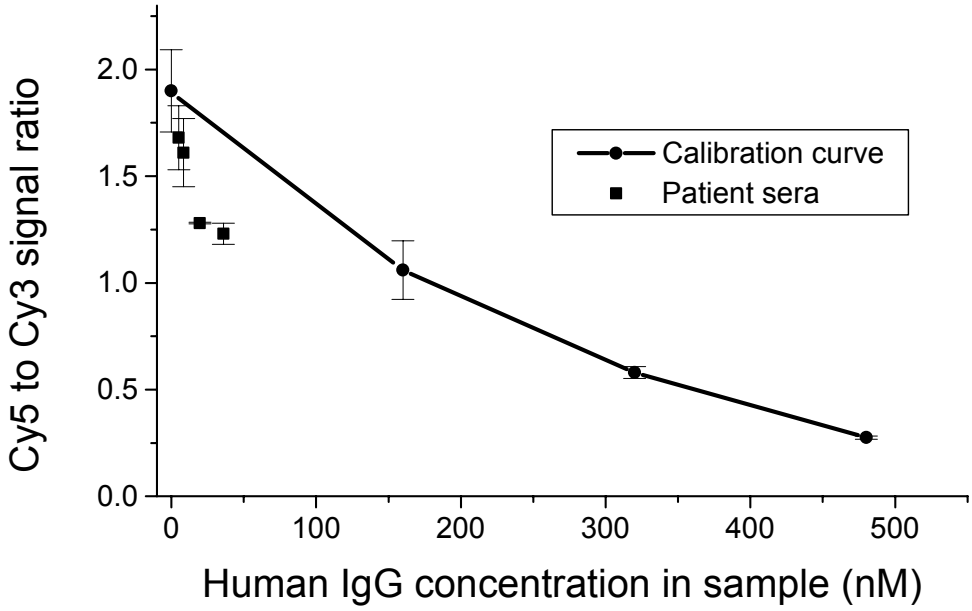

Figure 17: Concentration dependence obtained in TERASYS chips for human IgG in synthetic (circles, curve for the sake of clarity) and in serum (squares) samples.

Conclusion

Preliminary experiments showed that thermally aged PDMS was a more promising material than native or oxygen-plasma-treated elastomer. A simple coating procedure has been established to passivate the hydrophobic PDMS surface, while maintaining a residual surface charge capable of producing a modest EOF. The coating deposited in PDMS/glass microchannels is stable in biological fluids and detergent-free buffers. Strongly reduced adsorption (low NSB) makes its use possible for heterogeneous affinity assays. The coating concept enables integration of any biotinylated probe into the third layer. Moreover, the probe-patterning technique used in the channel network permits the quantification of bound target, NSB to the coated surface, and background fluorescence, on a single TERASYS device. Feasibility of an immunoreaction was demonstrated with an anti-human IgG/Cy5-human IgG system. The signal-to-noise ratio was found to be 206 for a sample containing 1.33 μM Cy5-human IgG, while labeled antigen NSB to the treated surface was effectively suppressed. Bound antigen quantification showed that fluorescence intensity was reproducible chip-to-chip and day-to-day. Data from eight disposable chips showed a relative chip-to-chip standard deviation of 18 %.

The anti-human IgG/Cy5-human IgG model used for immunoreactions was further developed into an immunoassay for human IgG. Performance of the assay was enhanced by the implementation of an internal standard. As a result, disposable microfluidic platforms for a heterogeneous competitive immunoassay of human IgG employing Cy5-human IgG as tracer and Cy3-mouse IgG as internal standard were obtained. Electrokinetic sample transport was applied in order to exploit a small difference between the net mobilities of analyte and tracer, thereby achieving a preconcentration of human IgG on the solid support that led to an increase in the sensitivity of the immunoassay at pH 9.3. The overall quality of the disposable chip and the performance of the immunoreaction were controlled by monitoring the fluorescence of the bound internal standard. Runs with abnormal internal standard response were discarded. Furthermore, data evaluation was based upon calculation of the ratio of fluorescence intensities of bound tracer and bound internal standard (Cy5-human IgG and Cy3-mouse IgG, respectively), an approach that reduced chip-to-chip variations. Using synthetic samples, the concentration dependence in

the range from 0 to 500 nM human IgG was shown to provide reproducible Cy5/Cy3 signal ratios between 2 and < 0.5, associated with an average RSD of 6.8 %. The incorporation of the internal standard is thereby demonstrated to provide the level of confidence required in clinical analysis. Furthermore, chips wet-stored at 4 °C over a two-month period were found to perform comparably to new chips, whereas dried chips stored at – 20 °C and re-hydrated prior to use could not be used at all.

The analysis of patient sera showed that the immunoassay platform behaved differently in the presence of serum-based samples. Using the same conditions as for the synthetic samples in the 0 – 500 nM range, no concentration dependence was noted. With a larger excess of tracer, a small dependence on IgG concentration was noted but did not permit exact quantification of IgG in these samples. However, patients with normal IgG levels (4.4 – 8.9 nM) could be clearly differentiated from patients with elevated IgG concentrations (10 - 50 nM).

Outlook

The data presented in this work shows that TERASYS can form the basis of a heterogeneous immunoassay for human IgG. The IgG immunoassay performed as described previously could potentially find an application in screening patients for elevated IgG levels. Real-time observation showed that the immunoreactions take place very quickly in the TERASYS chips, and that strong signals are obtained within 30 seconds. Therefore, the incubation time of the human IgG immunoassay could be shortened significantly. This aspect could be further exploited for a screening test.

In diagnostic labs, total IgG level is usually assessed by nephelometric assays. In a second stage, patient sera with high IgG levels are further tested for a gammopathy determination, which is carried out by immunofixation electrophoresis or immunoelectrophoresis. The latter analysis enables the distinction between cancer- and inflammation-related diseases. TERASYS chips cannot compete directly with the nephelometric assays. However, the concept could be adapted to carry out several parallel immunoassays, in a microfluidic system containing several intersections. The ability to pattern selectively each intersection with a specific antibody would allow a sample to be tested for many clinically relevant species at once, e.g. for gammopathy determination. Such a device would represent as a new tool in the diagnostics field, where a single chip could be used for screening patient, and at the same time carry out a gammopathy determination, see Figure 18. However, experiments showed that TERASYS chip response varied when changing from synthetic samples to serum-based samples. A new sample preparation protocol did not resolve this problem, though that a better understanding of the reasons for these variations will be required for a real application. Moreover, biotin-dextran in TERACOAT was replaced by biotin-IgG in TERASYS, without looking at the NSB suppressing capability of the new coating. A detailed study of the TERASYS surface seems would be appropriate.

Alternatively, the monitoring of pM antigen concentrations could be attained with longer incubation times, or by extending the delay between analyte and tracer delivery. Variation in the length of the sample delivery channel would be one simple way of controlling the start of sample addition.

Using the actual chip setup, the main drawback of the system is the fluorescence detection of the immunocomplex. Signal measurement accounts for about 50 % of the total analysis time (including channel coating). The high sensitivity achieved using the confocal microscope setup built into the array scanner is required to acquire the signal through the PDMS layer. However, the *z*-axis alignment of the collection lens is time consuming, and has to be repeated for each new structure because of the varying chip-to-chip PDMS thickness. Therefore, the use of an inverted setup, where light excitation and collection takes place through the bottom glass substrate would make the light path through the chip identical for all devices. Such a simplification of the optical detection would ultimately enable automated detection.

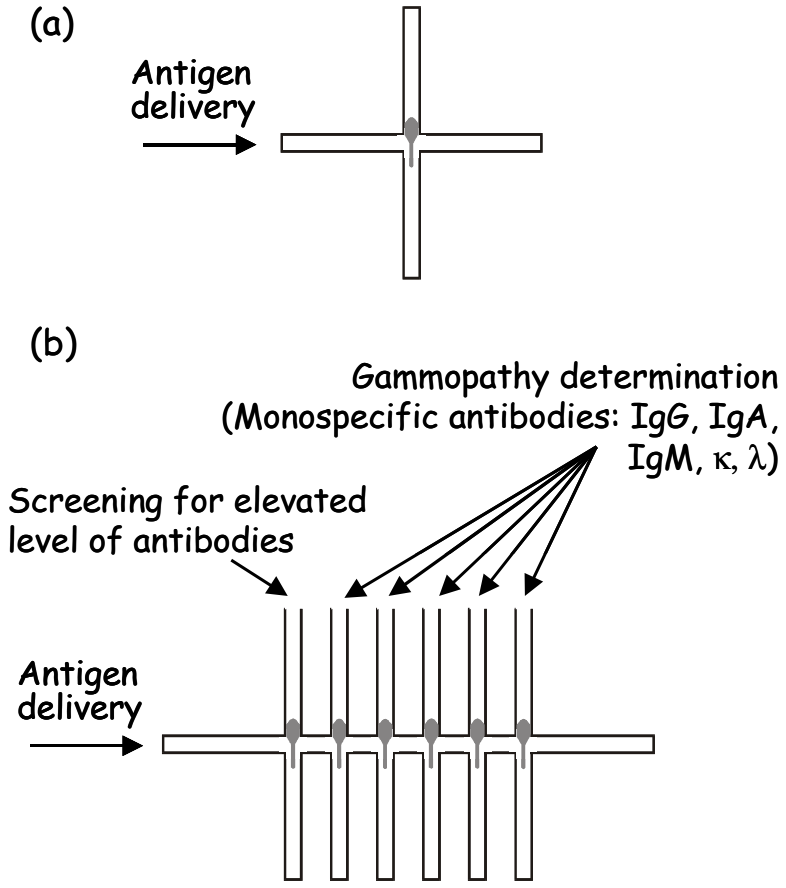

Figure 18: The TERASYS chip (a) concept could be modified into a fish bone-like channel network (b), where different antibodies are immobilized in each vertical channel. Serial sample delivery at each cross provides a chip for parallel immunoassays.

Acknowledgements

At this point, I would like to express my gratitude towards Dr. Elisabeth Verpoorte, Prof. Wolfgang Thormann and Dr. Hans Sigrist, who together assumed the supervision of my project. They spend countless hours teaching me Science, but also enlarged my vision of the sciences in many aspects such as ethics, politics, strategy, or marketing. Thanks also for your friendship and all these open discussions about traveling, career, gastronomy and everything else. You integrated me as a full member of your respective teams, which provided me with very enjoyable working conditions. Several times you gave me the opportunity to explore some of my ideas, and provided the framework that turned ideas into a successful microchip. You also made possible the interdisciplinary basis of this project, which I consider as the keystone of my PhD.

I would like to thank also all members of the three teams I worked with at IKP, IMT and CSEM, for their help in the lab, their time for listening and their friendship. I learned from you a lot about capillary electrophoresis, technology or surface chemistry and I will remember the very enjoyable time I spend with you in the lab.

At IKP, Dr. Andreas Ramseier, Dr. Sandra Zaugg, Dr. Anita Wey, Regula Theurillat, Jitka Caslavska, Francine Prost and Christian Lanz.

At IMT, Jan Lichtenberg, Laura Ceriotti, Dr. Antoine Daridon, Arash Dodge, Gian-Luca Lettieri, Rosanne Guijt, Mitra Trop and Jean-Christophe Roulet.

And at CSEM, Maria Juvet, François Crevoisier, Dr. Hui Chai-Gao, Isabelle Caelen Soury-Lavergne, Sylvie Guinchard, Odile Bucher, Dr. Eric Menotti, Dr. Martha Liley, Dr. Guy Voirin, Sylvia Angeloni, Eric Bernard, Réal Ischer, Dr. Rolf Eckert, Dr. J. Moritz Freiland, Dr. Harry Heinzelmann, Dr. Rino E. Kunz, Dr. Sylvia Jeney, Dr. Raphaël Pugin, Caterina Minelli, Kaspar Cottier and André Meister.

I wish to express my gratitude to Prof. Nico F. de Rooij who agreed to be my thesis supervisor at the University of Neuchâtel.

During these years, I also had the chance to work with many other people involved in many services ranging from the machine shop to the informatics group. Thanks to all for your support and advice.

Finally I would like also to thank my parents, friends, family and Isabelle for their long-standing support since I started thinking about chemistry years ago.

This project would not have been possible without the financial support of the Centre Suisse d'Electronique et de Microtechnique SA.

References

(1) Manz, A.; Graber, N.; Widmer, H. M. *Sens. Actuators B1* **1990**, 244-248.

(2) Harrison, D. J.; Fluri, K.; Seiler, K.; Fan, Z.; Effenhauser, C. S.; Manz, A. *Science* **1993,** *261*, 895-897.

(3) Jacobson, S. C.; Culbertson, C. T.; Daler, J. E.; Ramsey, J. M. *Anal. Chem.* **1998,** *70*, 3476-3480.

(4) Jacobson, S. C.; McKnight, T. E.; Ramsey, J. M. *Anal. Chem.* **1999,** *71*, 4455-4459.

(5) Hosokawa, K.; Fujii, T.; Endo, I. *Anal. Chem.* **1999,** *71*, 4781-4785.

(6) Salimi-Moosavi, H.; Tang, T.; Harrison, D. J. *J. Am. Chem. Soc.* **1997,** *119*, 8716-8717.

(7) Woolley, A. T.; Hadley, D.; Landre, P.; DeMello, A. J.; Mathies, R. A.; Northrup, M. A. *Anal. Chem.* **1996,** *68*, 4081-4086.

(8) Li, P. C. H.; Harrison, D. J. *Anal. Chem.* **1997,** *69*, 1564-1568.

(9) Kutter, J. P. *Trends in Anal. Chem.* **2000,** *19*, 352-363.

(10) Bruin, G. J. M. *Electrophoresis* **2000,** *21*, 3931-3951.

(11) Jacobson, S. C.; Moore, A. W.; Ramsey, J. M. *Anal. Chem.* **1995,** *67*, 2059-2063.

(12) Harrison, D. J., Glavina, P. G., Manz, A. *Sens. Actuators B* **1993**, *10*, 107

(13) Effenhauser, C. S.; Bruin, G. J. M.; Paulus, A.; Ehrat, M. *Anal. Chem.* **1997,** *69*, 3451-3457.

(14) Duffy, D. C.; McDonald, J. C.; Schueller, O. J. A.; Whitesides, G. M. *Anal. Chem.* **1998,** *70*, 4974-4984.

(15) McDonald, J. C.; Duffy, D. C.; Anderson, J. R.; Chiu, D. T.; Wu, H.; Schueller, O. J.; Whitesides, G. M. *Electrophoresis* **2000,** *21*, 27-40.

(16) McCormick, R. M.; Nelson, R. J.; Alonsoamigo, M. G.; Benvegnu, J.; Hooper, H. H. *Anal. Chem.* **1997,** *69*, 2626-2630.

(17) Locascio, L. E.; Perso, C. E.; Lee, C. S. *J. Chromatogr.* **1999,** *857*, 275-284.

(18) Martynova, L.; Locascio, L. E.; Gaitan, M.; Kramer, G. W.; Christensen, R. G.; MacCrehan, W. A. *Anal. Chem.* **1997,** *69*, 4783-4789.

(19) Barker, S. L.; Tarlov, M. J.; Canavan, H.; Hickman, J. J.; Locascio, L. E. *Anal. Chem.* **2000,** *72*, 4899-903.

(20) Gale, M. T. *Microelectron. Eng.* **1997**, *34*, 321-339

(21) Jacquier, J. C.; Rony, C.; Desbene, P. L. *J. of Chromatogr. A* **1993**, *652*, 337-345.

(22) Manz, A.; Effenhauser, C. S.; Burggraf, N.; Harrison, D. J.; Seiler, K.; Fluri, K. *J. Micromech. Microeng.* **1994,** *4*, 257-265.

(23) Huang, X.; Gordon, M. J.; Zare, R. N. *Anal. Chem.* **1988,** *60*, 1837-1838.

(24) Yalow, R. S.; Berson, S. A. *J. Clin. Invest.* **1960,** *39*, 1157-75.

Appendix I

Surface Bio-Passivation of Replicated PDMS Microfluidic Channels and Application to Heterogeneous Immunoreaction with On-chip Fluorescence Detection

Vincent Linder[1,2,3], Elisabeth Verpoorte[2], Wolfgang Thormann[3,*],

Nico F. de Rooij[2], Hans Sigrist[1]

[1] Centre Suisse d'Electronique et de Microtechnique SA (CSEM SA), CH-2007 Neuchâtel, Switzerland

[2] Samlab, Institute of Microtechnology, University of Neuchâtel, CH-2007 Neuchâtel, Switzerland

[3] Department of Clinical Pharmacology, University of Bern, CH-3010 Bern, Switzerland

Anal. Chem., **2001**, 73, 4181-4189.

Analytical Chemistry publisher denied the permission to add this appendix. Please refer to the published article to more details (see reference above)

Appendix II

Application of Surface Biopassivated Disposable PDMS/Glass Chips to a Heterogeneous Competitive Human Serum IgG Immunoassay with Incorporated Internal Standard

Vincent Linder[1,2,3], Elisabeth Verpoorte[2], Nico F. de Rooij[2],
Hans Sigrist[1], Wolfgang Thormann[3,*]

[1] Centre Suisse d'Electronique et de Microtechnique (CSEM), CH-2007 Neuchâtel, Switzerland

[2] SAMLAB, Institute of Microtechnology, University of Neuchâtel, CH-2007 Neuchâtel, Switzerland

[3] Department of Clinical Pharmacology, University of Bern, CH-3010 Bern, Switzerland

Electrophoresis, **2002**, 23, 740-749

ABSTRACT

A microfluidic platform for a heterogeneous competitive immunoassay of human immunoglobulin G (IgG) employing Cy5-human IgG as tracer and Cy3-mouse IgG as internal standard was developed. The device consisted of microchannels made of poly(dimethylsiloxane) and glass which were patterned with antibodies against human IgG and mouse IgG. Electrokinetic sample transport was employed in order to exploit the small difference between the net mobilities of analyte and tracer, thereby achieving favorable conditions for the performance of the competitive immunoreaction. The overall quality of the disposable chip and performance of the immunoassay were controlled by monitoring the fluorescence of bound tracer and bound internal standard. Analyses with an insufficient internal standard response were discarded, and immunoassay data evaluation was based on the ratio of tracer and internal standard fluorescence. Using synthetic samples in the range from 0 to 80 µg/mL IgG and alkaline running conditions, a concentration-dependent

response with reproducible Cy5/Cy3 signal ratios (average RSD of 6.8 %) was obtained. Chips stored with solution in the channels at 4 °C over a two-month period were found to perform like freshly prepared chips, whereas chips stored dry at – 20 °C and rehydrated prior to use could not be employed. The analysis of patient sera showed that the immunoassay platform behaved differently in the presence of serum-based samples. Using the same conditions as for the synthetic samples, no concentration dependence was noted. With a large excess of tracer, however, an IgG concentration dependence was observed, permitting distinction of samples of patients with normal IgG levels (8-16 mg/mL) from those with elevated IgG concentrations (> 16 mg/mL).

1 INTRODUCTION

Monitoring of immunoglobulin G (IgG) in serum is of clinical relevance. IgG concentrations between 8 and 16 mg/mL are considered normal, whereas elevated levels may be associated with chronic infection (polyclonal elevations) or cancer (monoclonal elevations). Thus, methods to monitor the total amount of IgG and to allow the distinction between polyclonal and monoclonal gammopathies are required [1]. In the past, many techniques have been employed for monitoring total human IgG in body fluids, including radial immunodiffusion and electroimmunoassays (also known as rocket immunoassays), methods that rely on precipitation reactions between antigen and antibodies [1]. Nowadays, quantification of IgG is carried out by nephelometric or turbidimetric immunoassays, techniques that are fast, automated and reproducible. Furthermore, different types of sandwich immunoassays for IgG have been described using various antibody labels, such as alkaline phosphatase [2], radioactive isotopes [3], and fluorophores [4]. Another approach reported relies on affinity chromatography using a fused-silica capillary packed with protein G coated beads [5]. Monoclonal gammopathies are assessed by either immunoelectrophoresis or immunofixation electrophoresis. These semi-quantitative approaches enable distinction between a monoclonal, an oligoclonal and a polyclonal gammopathy. During the past decade, analysis of serum proteins by capillary zone electrophoresis has been introduced and applied to the monitoring of monoclonal IgG using immunosubtraction [6,7].

Starting in the early 90's with the integration of capillary electrophoresis techniques onto glass chips, an increasing number of applications have been implemented on microfluidic platforms with the goal of developing configurations for high-throughput or point of care analyses. Among these developments, the performance of homogeneous immunoassays in microfluidic-based instrumentation has been investigated and applied to the analysis of cortisol [8] and theophylline [9,10] in serum. Mouse IgG has been analyzed on planar glass structures using enzyme-labeled anti-mouse antibodies and chemiluminescence detection [11]. Competitive heterogeneous immunoassays for the pregnancy hormone chorionic gonadotropin and theopylline have been implemented in microchannels using evanescent field detection [12]. In a different approach, secretory human immunoglobulin A [13] and carcinoembryonic antigen [14] have been analyzed on polystyrene micro-beads clustered

behind a dam microfabricated in a microfluidic channel. Poly(dimethylsiloxane) (PDMS) microchannel surfaces have been modified with phospholipids for the detection of anti-dinitrophenyl antibodies [15] or with proteins for sheep IgM quantification by an ELISA [16]. Similarly, a Pyrex microfluidic reaction chamber has been modified with protein A in order to produce a platform for IgG binding, which has been used for rabbit IgG detection in buffer [17]. Surface patterning has been applied to PDMS, thereby enabling micromosaic immunoassays to be carried out for chicken IgG [18], or providing a surface for human IgG binding [19].

In previous work from our laboratories, PDMS/glass chips featuring a surface treatment comprised of a three-layer, biotin-neutravidin-based sandwich coating were developed and applied to an electrokinetically driven, heterogeneous immunoreaction for human IgG [19]. Continuation of this project was geared towards the performance of an immunoassay for human IgG on a disposable PDMS/glass chip. For that purpose, incorporation of an internal standard, electrokinetic sample delivery and analysis of synthetic and patient samples were studied. The data presented in this paper are the first results of a heterogeneous competitive immunoassay for human IgG performed on disposable, surface biopassivated PDMS/glass chips and thereby demonstrate the feasibility of developing microfluidic platforms for the rapid determination of elevated IgG levels in human serum.

2 MATERIALS AND METHODS

2.1 Materials and reagents

Microscope slides 26x76 mm^2 made of polished AF45-glass were purchased from Schott Schleiffer (Feldbach, Switzerland). The Dow Corning PDMS kit Sylgard 184 was obtained from Distrelec (Nänikon, Switzerland). The Cy5 antibody labeling kit was purchased from Amersham Pharmacia Biotech (Dübendorf, Switzerland). Biotin-conjugated dextran (10 kDa) and neutravidin were Molecular Probes products purchased from Juro Supply (Luzern, Switzerland). Biotin-conjugated goat anti-mouse IgG and biotin-conjugated goat anti-human IgG were manufactured by Pierce (Rockford, IL, USA) and obtained from Socochim (Lausanne, Switzerland). Purified human IgG was obtained from ICN Biomedicals GmbH (Eschwege, Germany). Cy3-conjugated mouse IgG was manufactured by Jackson Immunoresearch Laboratories (West Grove, PA, USA) and purchased from Milan Analytica (La Roche, Switzerland). Other reagents were of research grade. PBS

refers to phosphate buffer saline containing 50 mM phosphate buffer (pH 7.4) and 150 mM NaCl. Biotin-conjugated goat anti-mouse IgG contained bovine serum albumin which was removed as described in [19] using protein G-coated Sepharose beads (Fast Flow 4B; Sigma, Buchs, Switzerland) and PD-10 columns prepacked with Sephadex G-25M (Amersham Pharmacia Biotech).

2.2 Tracer and sample preparation

The tracer, Cy5-labeled human IgG, was prepared according to the manufacturer's instructions, using the antibody-labeling kit comprising NHS-activated Cy5 dye. By varying the initial amounts of human IgG and/or activated dye in the reaction vial, 2 to 9 Cy5 molecules could be attached to each IgG molecule. Two batches of Cy5-human IgG were used in this study (referred to as batches I and II), having a dye-to-protein molar ratio of 2.2 and 2.9, respectively. The extent of labeling was determined according to the manufacturer's instructions using UV/VIS spectroscopy.

Synthetic samples employed to evaluate the concentration dependence of the immunoassay at physiological and alkaline conditions were prepared from 200 μg/mL solutions of Cy3-mouse IgG (internal standard), unconjugated human IgG, and Cy5-human IgG (batch I and II, tracer) in PBS. If not stated otherwise, unconjugated human IgG and Cy5-human IgG were mixed to obtain solutions comprising analyte/tracer ratios of 0, 0.125, 0.250, 0.500 and 0.800. Finally, 200 μL of the latter solution was mixed with 200 μL of Cy3-mouse IgG. Human serum samples were prepared differently. Serum was diluted 150 times with PBS, and 5 μL of diluted serum was mixed with 195 μL of Cy5-human IgG solution (batch II). Then, 25 μL of the latter solution was mixed with 25 μL of Cy3-mouse IgG. The total serum dilution was 12'000-fold. Depending on the human IgG concentration in serum, the total IgG concentration (IgG stemming from serum, tracer and internal standard) in the final sample varied between 198 and 202 μg/mL. Matrices of synthetic and serum samples were essentially the same (100 % and 99.9 % PBS, respectively).

2.3 PDMS/glass chip preparation

Preparation of the PDMS/AF-45 glass devices has been described elsewhere [19]. Briefly, the channel design (see Fig. 1) was transferred onto a silicon wafer by photolithographic techniques. The master for PDMS replication was obtained by deep reactive ion etching of

the wafer where it was not coated by photoresist. Liquid PDMS pre-polymer was poured onto the silicon master and cured 4 h at 65°C. Polymerized PDMS replicas of about 0.8 mm thickness were peeled off, and at the channel ends, 4-mm access holes were punched out using a cork borer. Prior to reversible sealing with an AF45-glass slide, replicas were thermally treated at 115°C for 12 h, and cleaned in isopropanol and water.

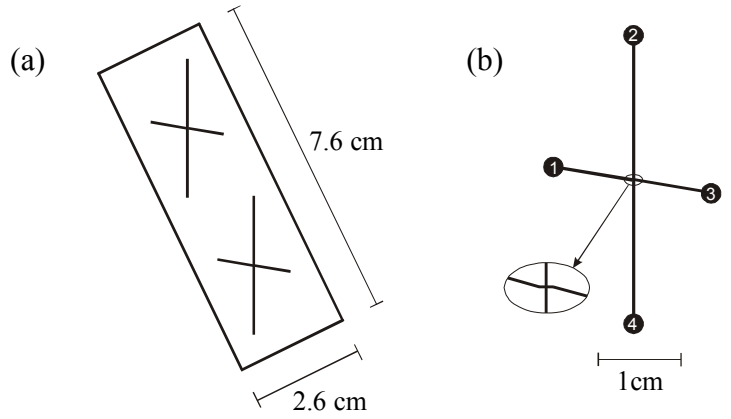

Fig. 1: (a) Overall schematic representation of the PDMS/AF-45 glass device and (b) detailed representation of the individual cross-like channel layout. Channel dimensions were 90 µm wide and 8 µm deep (rectangular profile). To prevent electrical short circuits between electrodes, the distance between reservoirs was increased by bending the two side branches of the cross.

Biochemical surface treatment was carried out in order to suppress non-specific binding (NSB) to the PDMS surface and to permit immobilization of specific antibodies in a sensing area located at the cross-shaped intersection of the microchannels. As previously described [19], a three-layer coating called TERASYS (TERnary Affinity SYStem) that relies on a biotin-neutravidin-biotin sandwich was applied. A ground layer of biotin-conjugated mouse IgG was physisorbed onto the PDMS and glass surfaces, followed by a second layer of neutravidin. In the third layer, the channel network was partially coated with biotinylated antibodies to be used later for the immunoassay, and the remaining area was coated with inert biotin-conjugated dextran. The spatial resolution of the immobilized biomolecules was achieved using a flow patterning technique. Reservoirs 1 and 3 (numbering according to Fig. 1b) were filled with a solution of biotin-conjugated dextran, and a solution containing biotinylated antibodies was pipetted into reservoir 4. Suction

pumping at reservoir 2 generated three converging laminar flows toward vacuum. Biotinylated species attached to the neutravidin surface according to the flow profiles. Thus, a strip of antibodies was immobilized between reservoirs 4 and 2, while side channels were covered with dextran (as shown in Fig. 2a and Fig. 3a).

2.4 Instrumentation for electrokinetically driven immunoassay

The chip was mounted on a custom-made PMMA holder that fitted onto the XY table of an inverted fluorescence microscope (Axiovert S 100; Carl Zeiss, Zürich, Switzerland). Optics located below the table enabled qualitative observation during the assay. A detailed description of this instrumentation has been reported elsewhere [19]. Briefly, fluorescence microscope observation was possible at different wavelengths, using the available set of filters for fluorescein (blue light excitation), Cy3 (green) or Cy5 (red). The emission light was focused on a CF 8/4 DXC black-and-white CCD camera (Kappa, Gleichen, Germany). Above the chip, platinum electrodes ensured electric connection to the high voltage (HV) supply. A custom-made HV power source assembled by Goeckeler Electronique (Neuchâtel, Switzerland) was controlled by two DAQPad-6020E boards from National Instruments (Austin, TX, USA). The overall system was computer-controlled, using in-house software written in Labview (National Instruments).

2.5 Competitive heterogeneous immunoassay conditions for human IgG

Immunoassay conditions at physiological pH (PBS, pH 7.4) and at alkaline pH (50 mM sodium tetraborate buffer, pH 9.3) were investigated (Fig. 2). TERASYS chips were conditioned with the appropriate buffer by maintaining a suction driven flow of buffer throughout the network during 1 min. Fig. 2 outlines schematically how antibodies were patterned onto the channel surfaces at the intersection, and how the immunoassay was subsequently carried out at physiological or alkaline pH. The large arrows in panels b) to e) indicate the direction of the electrokinetic transport of the antigens. It should be noted that at pH 7.4, the electrophoretic mobility of the negatively charged human IgG was large enough that it determined the overall transport direction of this species, which was opposite to the electroosmotic flow (EOF). At pH 9.3, the apparent mobility of human IgG was in the direction of EOF. When working with PBS, sample was pipetted into reservoir 3, and electrokinetically transported towards reservoir 1 using a high electric field. Incubation at a much reduced electric field and a washing step followed.

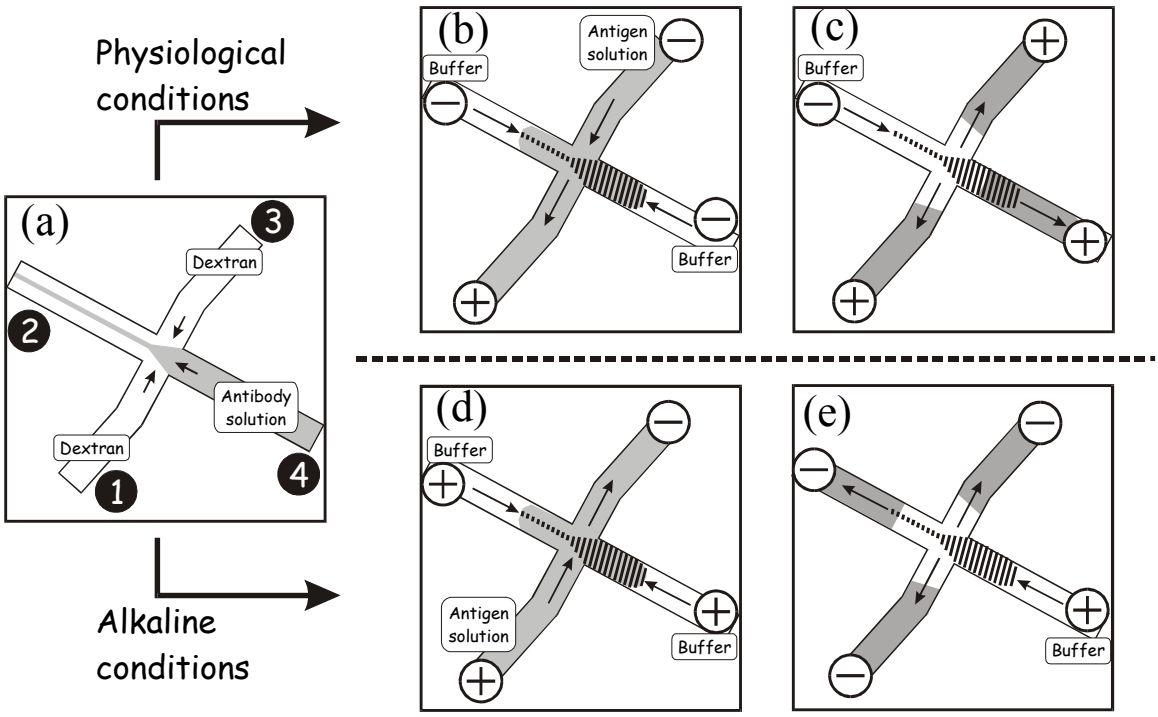

Fig. 2: Schematic representation of the flow patterns and antigen transport for the IgG immunoassay. For the sake of clarity, the polarities (+, -) at the reservoirs are given relative to the electric potential at the channel intersection. Small arrows in panel a) mark the direction of pressure driven flow, whereas the large arrows in panels b) to e) indicate the direction of the electrokinetic transport of the antigens. (a) Bioprobe patterning: the biotin-conjugated antibodies were immobilized on the neutravidin-coated surface. The immobilization pattern followed the laminar flow profiles generated by vacuum pumping at reservoir 2. (b),(c) Under physiological conditions, the immunoreaction took place at the intersection where antibodies were immobilized and in contact with sample (hatched area). (b) Sample (antigen) was electrokinetically delivered across the antibody-coated area. Side buffer flow was kept much smaller than sample flow, such that no flow patterning was observed at the cross. Sample was delivered to the intersection under an electric field of 300 Vcm-1 (75 s; -600 V at reservoir 3, -420 V at reservoirs 2 and 4, ground at reservoir 1). Incubation was carried out under an electric field of 60 Vcm-1 (360 s; -120 V, -84 V and 0 V at reservoirs 3, 2/4 and 1, respectively). (c) Unbound antigen was removed by electrokinetic pumping (60 s; -72 V at reservoirs 1 and 3, -600 V at reservoir 2, ground at reservoir 4) without removing the bound antigen (hatched area). (d), (e) Under alkaline (pH 9.3) conditions, the same immunoreaction was carried out at the intersection. (d) Sample was electrokinetically transported across the immobilized antibodies and incubated with an electric field of 275 Vcm-1 (400 s; -600 V at reservoir 3, -120 V at reservoirs

2 and 4, ground at reservoir 1). (e) Unbound antigen was then washed away (60 s; -600 V at reservoirs 1, 2 and 3, and ground at reservoir 4). All reservoirs were finally rinsed with running buffer.

Incubation and immunocomplex formation of Cy5-human IgG in a TERASYS chip at physiological conditions was observed using fluorescence microscopy (Fig. 3b and 3c). In case of alkaline conditions, sample was loaded into reservoir 1 and transport occurred towards reservoir 3 (no reduction of the electric field during incubation), followed by a washing step. A detailed description of the experimental conditions used for the two immunoassay formats is given in the legend of Fig. 2.

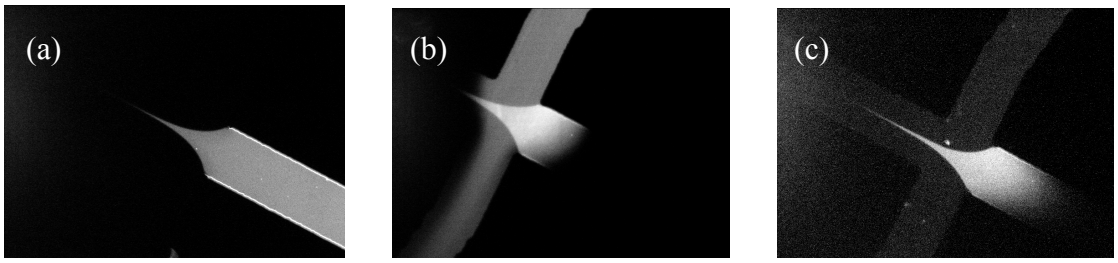

Fig. 3: Step-by-step observation of the immunoreaction at physiological pH by fluorescence microscopy. (a) Antibodies are patterned on the neutravidin surface using laminar flows. Immobilized antibodies used in TERASYS chips are not fluorescently labeled. For taking this picture, however, Cy3-biotin-conjugated antibodies were used for observation purposes only. (b) Fluorescently labeled antigen is electrokinetically transported towards the immobilized antibodies of the TERASYS chip, where the heterogeneous immunoreaction takes place (brighter area at channel intersection). (c) Unbound antigen is electrokinetically removed, and fluorescence arising from the immunocomplex can be quantified.

2.6 On-chip fluorescence detection

Quantitative measurements were carried out using a Model 428 Array Scanner (Affymetrix, Santa Clara, CA, USA). This scanner comprises a confocal microscope that is designed for fluorescence measurements on substrates the size of a microscope slide, and has 10-µm pixelation. TERASYS chips were held on a mechanical stage and moved beneath an oscillating lens. The excitation light was focused on the channel and emission light was collected back through the PDMS replica. Observation through the PDMS layer changed the focus point location beyond the possible working range of the lens adjustment

mechanism. Thus, proper alignment in the z direction was achieved by increasing the substrate thickness using strips of tape 200 µm thick applied along the edges of the device on the glass side, as is illustrated in Fig. 4.

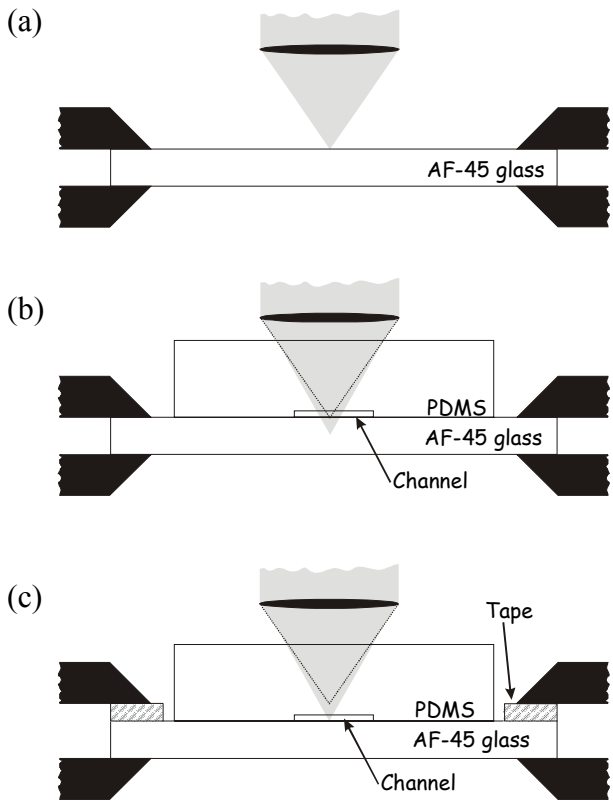

Fig. 4: Schematic illustration of the z direction alignment used for on-chip fluorescence detection. (a) A microscope slide is clipped onto the mechanical stage using holders (black). Excitation light (grey) is focused on the slide surface by adjustment of the lens. (b) The excitation light trajectory is changed by refraction when entering PDMS so that the focal point position is shifted beneath the channel. The dotted line represents the original light trajectory in absence of PDMS. The focal point shift is outside the range of the lens adjustment. (c) Addition of a 200 µm thick layer of tape (hatched areas) on the edges of the slide compensates for the focal point displacement.

This effectively lowered the channel to fall into the focal plane of the lens. Fine adjustment of the focal point was necessary to take into account the changes of the PDMS thickness. Two scans were carried out in the region of interest using 532 and 650 nm diode lasers. The average fluorescence intensity at 570 nm (Cy3) and 665 nm (Cy5) was quantified

individually for each scan across a circular area with 3 pixels (30 μm) in diameter using an image processing software (Imagene 4.01, Biodiscovery, Los Angeles, CA, USA).

3 RESULTS AND DISCUSSION

3.1 Incorporation of an internal standard into the TERASYS platform

A clinical diagnostic test requires a high level of confidence in the results obtained. TERASYS chips described in this contribution are single-use disposable devices that cannot be calibrated or tested prior to use. Systematic control of the chips by optical microscopy may provide quality control during microfabrication steps. Similarly, TERASYS surface modification may be controlled by electrokinetic characterization [19]. Immobilized antibody activity and sample transport in the chip, however, cannot be controlled by these methods. Thus, the overall quality of the chip and the success of the immunoreaction were controlled using an internal standard that was implemented into the TERASYS platform. The third layer of the coating, where antibodies for recognition are located, was prepared with two different antibodies. Biotin-conjugated anti-mouse IgG and biotin-conjugated anti-human IgG were co-immobilized by flushing a 1:1 solution during the patterning step, while biotin-conjugated dextran was used for passivation of the side channels. At that stage, mass transport relied on suction pumping. Biotinylated antibodies were assumed to be bound in equal quantities to the neutravidin surface, and thus were equally reactive towards both IgG's. A possible discrimination originating from unequal electrokinetic transport could thus be excluded.

Samples subjected to the competitive immunoassay for human IgG contained Cy5-human IgG and Cy3-mouse IgG as tracer and internal standard, respectively. Cy3 and Cy5 conjugates (for structures see Fig. 5) can be spectrally distinguished (excitation/emission at 532/570 nm and 650/665 nm, respectively). The emission light of Cy3 (570 nm) cannot excite Cy5 and the fluorescence of Cy3 and Cy5 can thus be individually quantified. All samples were prepared with a fixed amount of Cy3-mouse IgG, which was equal to the total quantity of human IgG and Cy5-human IgG. The Cy5-to-Cy3 fluorescence signal ratio was determined and employed as the basis for data evaluation. Abnormal or lack of Cy3 signal showed that the TERASYS chip was not working properly (see below), while minor chip-to-chip variations were compensated for by using the signal ratio. Variations occurring from channel replication problems or surface chemistry are balanced by the co-

immobilization of the two antibodies. A TERASYS platform of low anti-human IgG content will show a proportional reduction of immobilized anti-mouse IgG as well.

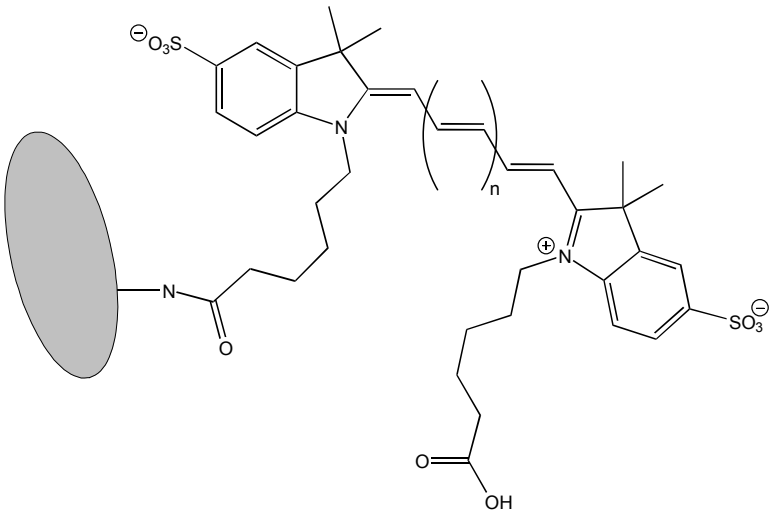

Fig. 5: Chemical structure of Cy3 (n=0) and Cy5 (n=1) labels after attachment to an IgG molecule (grey ellipse). The diagram is not to scale, since in reality IgG is about 200 times larger than the label

3.2 Electrokinetic sample transport and elucidation of the IgG concentration dependence

For execution of the immunoassay in TERASYS chips, unconjugated and fluorescently labeled IgG's were electrokinetically transported to the reactive area. At physiological pH, Cy3-mouse IgG and Cy5-human IgG were shown by fluorescence microscopy to be displaced towards the anode, i.e. against the EOF. The opposite behavior was observed in channels conditioned with 50 mM tetraborate buffer at pH 9.3, where the net displacement occurred in the direction of the cathodic EOF. Identical behavior was indirectly observed for unconjugated human IgG. For both cases, electrokinetic mass transport was very slow, indicating that electroosmotic and electrophoretic contributions to the observed IgG mobilities were similar. The net mobility of Cy3-mouse IgG was determined to be in the range of $5 \cdot 10^{-5}$ to $8 \cdot 10^{-5}$ $cm^2 s^{-1} V^{-1}$. At physiological and alkaline conditions (pH 7.4 and 9.3 respectively), polyclonal IgG molecules are negatively charged. However, the exact charges are unknown. Introduction of Cy3 or Cy5 labels on an IgG molecule (see Fig. 5) increases the number of negative charges and the electrophoretic mobility of labeled IgG is

expected to be slightly higher compared to that of unconjugated IgG. As the net transport of IgG was found to be low (close to balance of electroosmotic and electrophoretic fluxes), relatively small changes of either of the electrokinetic contributions could have a significant impact on net solute mobility.

In PBS conditioned chips, IgG's were found to be displaced towards the anode (against EOF, Fig. 2b) and the more negatively charged molecules were thus transported faster. When a competitive immunoassay was carried out using the human IgG/Cy5-human IgG system, the labeled partner arrived first to the area comprising the immobilized anti-human antibodies. By the time unconjugated human IgG reached the immobilized antibodies, most of the binding sites were already occupied by the Cy5-human IgG. It appeared that only a small fraction of the binding sites were left available for competition. Therefore most of the large fluorescence signal recorded was irrelevant for the human IgG-to-Cy5-human IgG ratio in the sample. Hence, the competitive immunoassay was almost concentration independent (see Fig. 6). In contrast, in the alkaline medium, IgG's were electrokinetically displaced towards the cathode (direction of EOF) and the less negatively charged molecules were transported faster to the immunochemical reaction site.

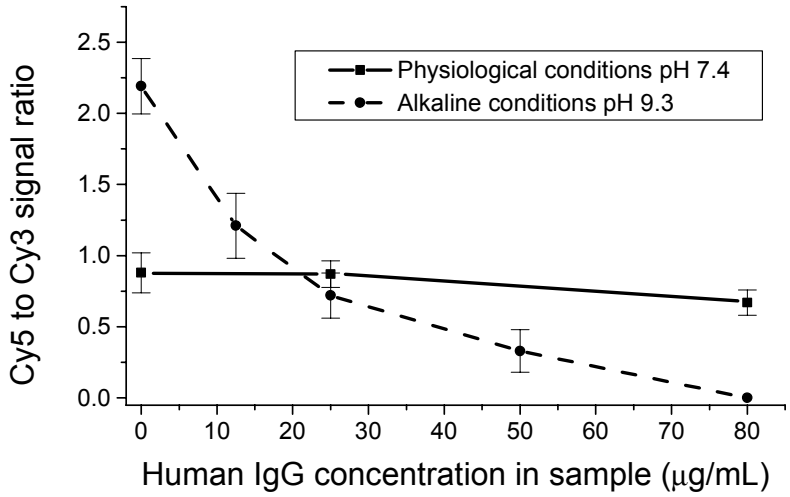

Fig. 6: Concentration dependence of the competitive immunoassay assessed via use of synthetic samples comprising varying relative amounts of human IgG / Cy5-human IgG (batch I). Experiments conducted at physiological pH (squares, solid line) showed almost no concentration dependence, while good sensitivity was obtained for experiments carried out under alkaline conditions (circles, broken line).

Unconjugated human IgG reached the immobilized antibodies first and could be bound to the anti-human IgG without competition until Cy5-human IgG arrived as well. Samples of high human IgG content were able to bind almost all sites before arrival of Cy5-human IgG, yielding a very low fluorescence signal. On the other hand, only a few sites were bound by human IgG upon analysis of samples of low human IgG content. At the time Cy5-human IgG arrived, plenty of sites were still available, with little competition due to the high relative concentration of labeled species in the sample. Thus, due to the pre-concentration of unlabelled species occurring during the first stage of the immunoassay, this assay format appeared far more sensitive to the human IgG concentration in the sample (Fig. 6). Taking advantage of the enhanced sensitivity at alkaline pH, the human IgG limit of detection of the calibration system was estimated to be around 5 µg/mL. At that pH, electrokinetic transport of labeled IgG could be shown to be extremely sensitive to the number of additional negative charges. Optimal labeling appeared to be in the range of 2 to 3 Cy5 dyes per IgG molecule. A lower degree of labeling yielded a weaker fluorescent signal for the bound Cy5-human IgG at the reactive site, and reduced the assay sensitivity. Cy5-human IgG with a labeling degree higher than 3 was shown not to be electrokinetically transported to the immunochemically reactive site.

The activity of a second batch of Cy5-human IgG (batch II) was tested by running a concentration dependence under alkaline assay conditions only. With four synthetic samples comprising analyte/tracer ratios of 0, 0.25, 0.50 and 0.75, a total of 11 chips were analyzed. From all data points, only one appeared to be out of the expected range. The internal standard value for that measurement was 9900 A.U., whereas the measured response for the other ten chips was > 13'000 A.U. Thus, the data of TERASYS chips showing an internal standard signal below 13000 A.U. were discarded. The concentration dependence obtained using Cy5-human IgG batch II provided a somewhat smaller sensitivity for human IgG compared to the results obtained with batch I (Fig. 7).

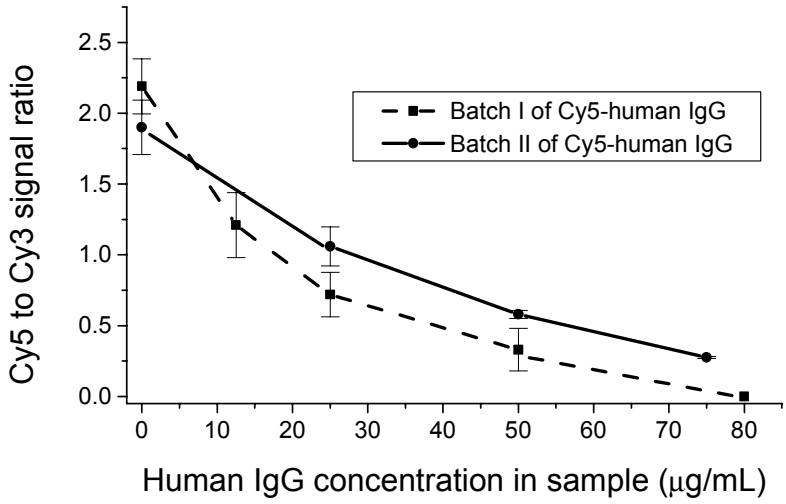

Fig. 7: Concentration dependence for human IgG using batch II of Cy5-human IgG (labelling ratio of 2.9) in comparison to batch I of Cy5-human IgG (labelling ratio of 2.2).

3.3 IgG monitoring in human serum

For the determination of IgG in human serum, an assay with a calibration range between about 5 and 100 mg/mL is required. Using the experimental conditions that led to the data presented in Fig. 7 for analysis of human serum, concentration-independent data were obtained. Thus, the four sera obtained from the clinical chemistry laboratory of the Inselspital (Bern, Switzerland) with reported IgG levels of 9.2 mg/mL, 15.3 mg/mL, 35.5 mg/mL and 64.7 mg/mL (determined using the BNII nephelometric immunoassay of Dade Behring) were prepared with a large excess of tracer (cf. section 2.2; analyte/tracer ratios of 0.0079, 0.0131, 0.0303 and 0.0553, respectively) and each sample was analyzed on four freshly prepared TERASYS chips. From the 16 runs, the data of 6 chips were discarded due to the internal standard signals being too weak. Results obtained in the properly working TERASYS chips showed a concentration dependence for human IgG (Fig. 8). A plot of the data obtained with synthetic and serum samples on the same scale (Fig. 8b) showed that the human IgG concentration dependence was different. With the different sample preparation scheme applied for serum, changes in the TERASYS responses were expected. Despite the 12’000-fold dilution of serum, matrix effects appear not to be completely abolished. No work geared towards identification of the sources of these effects was undertaken.

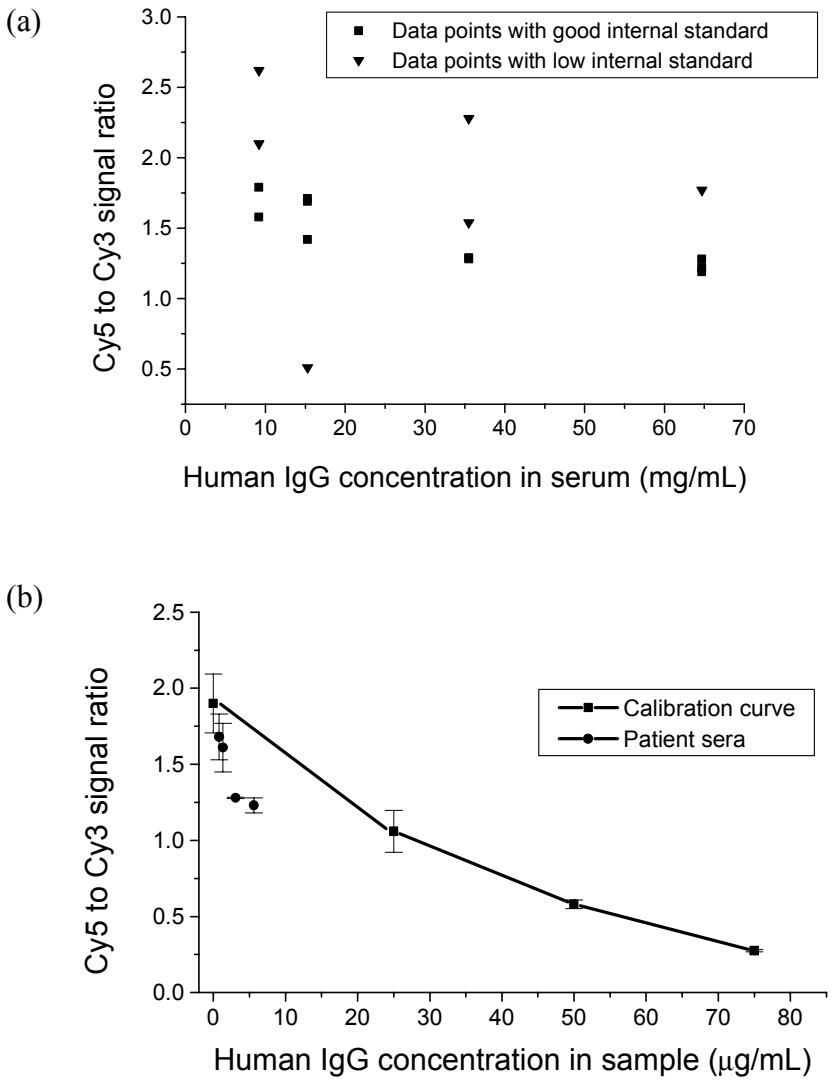

Fig. 8: Four patient sera were analyzed in a total of 16 TERASYS chips (4 each) using batch II of Cy5-human IgG. (a) From all results obtained, 6 data points were discarded (triangle; weak internal standard response). A concentration dependence for human IgG was noted for the data obtained in 10 properly working TERASYS chips (square). (b) Comparison of serum sample data with those obtained for synthetic samples containing the Cy5-human IgG (batch II) of Fig. 7.

One aspect to be evaluated would be the possible interaction of serum constituents with the channel walls (e.g. adsorption of serum proteins) which could lead to the perturbation of the electrokinetic delivery of analytes to the immunochemical reactive site. Quantification of human IgG in serum was found to be difficult, due to the high RSD at a low human IgG concentration and the small concentration dependence at higher IgG levels (Fig. 8).

However, the data obtained for the two patients with normal IgG levels can be clearly distinguished from the data of the two other patients, who had elevated IgG levels caused by a chronic infection (35.5 mg/mL) and cancer myeloma (64.7 mg/mL). The limit of detection for human IgG in serum samples was estimated at about 6 mg/mL which corresponds to an IgG sensitivity of 0.5 µg/mL in the 12'000-fold diluted sample. Thus, after elucidation of the unexplored aspects discussed above, this technology could be applied to the screening of patient sera with unambiguous recognition of elevated IgG levels.

3.4 Reproducibility and long term stability of TERASYS IgG chips

Clinical assays require a high level of confidence in the overall analysis process. This confidence in the result has been attained in the TERASYS chip thanks to the use of Cy3-mouse IgG as internal standard. In this study, the internal standard monitoring enabled the selection of the chips that worked properly throughout all steps from microfabrication to immunoassay. In the case of patient serum analysis, 6 TERASYS chips out of 16 were not qualified. As seen in Fig. 8a, without such a discrimination, no concentration dependence behavior could have been established. Moreover, the calculation of the Cy5-to-Cy3 ratio (tracer-to-internal standard ratio) enhanced the assay reproducibility. Recording the fluorescence signal arising from Cy5 led to RSDs of about 18 % [19]. The use of the Cy5/Cy3 signal ratio revealed an average RSD value of 6.8 % (RSD values for the Cy5-mouse IgG batch II data presented in Fig. 7 were determined to be between 1.8 and 13 %).

The long-term stability of fully prepared TERASYS chips was investigated using two means of chip storage. In a first series of chips, PBS was left in the microfluidic network and the chips were stored protected from light at 4°C. A second series of chips was conditioned with 100-fold diluted PBS and the reservoirs were emptied. Water in the channels was allowed to evaporate in a vacuum chamber (0.05 mbar) and the chips were stored protected from light at –20°C. The purpose of that procedure was to provide salts to the biomolecules, which is important for stabilizing the protein structure in absence of water. The dilution of PBS was required to avoid channel clogging due to crystallization of buffer constituents. After a two-month storage period, immunoassays using a 1:1 Cy3-mouse IgG/Cy5-human IgG solution (analyte/tracer ratio of 0) were performed under alkaline running conditions in both sets of chips. Ideally, data comparable to those for 0 µg/mL human IgG obtained in freshly prepared chips (first data points in Fig. 7) would

thus be obtained. Before use, dried chips were filled with PBS and rehydration of the biomolecules was allowed for 50 min at room temperature. Difficulties were encountered when PBS was introduced into the dried microchannels, mainly due to the formation of air bubbles. However, chips stored wet were conditioned with fresh PBS without any problem. Immunoassays carried out in these chips were found to perform well and reproducibly (Fig. 9a). The mean Cy5/Cy3 fluorescence intensity ratio was 2.07 (RSD = 8.1 %, n = 4, Cy5-human IgG batch II), a value that compares well with 1.94 (RSD = 6.25 %, n=3, Cy5-human IgG batch II) obtained in freshly prepared chips. However, the performance of electrokinetically driven immunoassays was not possible anymore in the reconstituted, dry-stored chips. Surface passivation did not survive the dry-storage treatment (Fig. 9b).

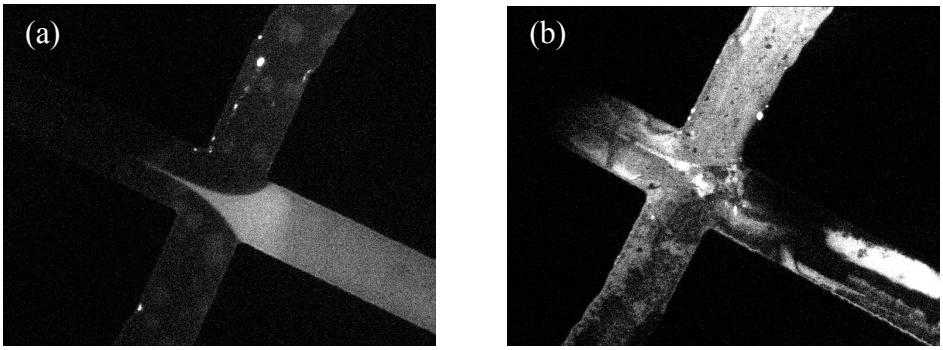

Fig. 9: Immunoassays under alkaline conditions in chips that were stored for a two-month period. (a) Assays could be performed nicely when the chips were wet-stored at 4°C and (b) could not be performed after dry storage at –20°C (surface passivation was damaged). Pictures were acquired by fluorescence microscopy.

4 CONCLUDING REMARKS

A disposable microfluidic platform for a heterogeneous competitive immunoassay of human IgG employing Cy5-human IgG as tracer and Cy3-mouse IgG as internal standard was developed in surface-biopassivated channels made of PDMS and glass. Employing pressure-driven hydrodynamic fluid flow, the surface of the microchannels was passivated with a three-layer coating and patterned with antibodies specific for human IgG (analyte) and mouse IgG (internal standard). Electrokinetic sample transport was applied in order to

exploit a small difference between the net mobilities of analyte and tracer, thereby achieving a preconcentration of human IgG on the solid support that led to an increase in the sensitivity of the immunoassay. The overall quality of the disposable chip and the performance of the immunoreaction could be controlled by monitoring the fluorescence of the bound internal standard. Runs with abnormal internal standard responses were discarded. Furthermore, data evaluation was based upon calculation of the ratio between fluorescence intensities of bound tracer and bound internal standard (Cy5-human IgG and Cy3-mouse IgG, respectively), an approach that reduces the impact of chip-to-chip variation. Using synthetic samples, the concentration dependence in the range from 0 to 80 µg/mL IgG was shown to provide reproducible Cy5/Cy3 signal ratios between 2 and < 0.5, values that vary slightly between different Cy5-human IgG batches and are associated with an average RSD of 6.8 %. The incorporation of the internal standard was therefore demonstrated to provide the level of confidence required in clinical analysis. Furthermore, chips wet-stored at 4 °C over a two-month period were found to perform similarly, whereas dried chips stored at – 20 °C and rehydrated prior to use could not be employed at all. The analysis of patient sera showed that the immunoassay platform behaved differently in presence of serum-based samples. Using the same conditions as for the synthetic samples, no concentration dependence was noted. With a large excess of tracer, a small dependence on IgG concentration was observed but did not permit exact quantification of IgG in these samples. Further work is required to properly elucidate the reasons leading to this behavior and to identify conditions yielding an increased concentration dependence. However, patients with normal IgG serum levels (8-16 mg/mL) could be clearly differentiated from patients with elevated IgG concentrations (> 16 mg/mL). Thus, these data show that TERASYS chips could be used for the rapid screening of patient sera. A more complex microchannel design containing multiple intersections with different immobilized specific antibodies (e.g. antibodies against IgG, kappa and lambda) could be developed and applied to the simultaneous on-chip monitoring of various parameters, including identification of a monoclonal gammopathy. This is an advantage compared to the use of capillary zone electrophoresis in which, after immunosubtraction with different antibodies applied to aliquots of serum, multiple experiments have to be performed [6].

ACKNOWLEDGEMENTS

V. Linder is a recipient of a CSEM university collaboration grant. The authors thank Dr. U. Marti for helpful discussions and for providing the patient sera.

5 REFERENCES

[1] Turgeon, M. L. *Immunology and Serology in Laboratory Medicine*, 2nd ed.; Mosby: St. Louis, 1996.

[2] Lamari, F., Anastassiou, E. D., Dimitracopoulos, G., Karamanos, N. K., *J. Pharm. Biomed. Anal.* 2000, *23*, 939-946.

[3] Klein, F., Skvaril, F., Vermeeren, R., Vlug, A., Duimel, W.J., *Clin. Chim. Acta* 1985, *150*, 119-127.

[4] Sun, B., Xie, W., Yi, G., Chen, D., Zhou, Y., Cheng, J., *J. Immunol. Methods* 2001, *249*, 85-89.

[5] Wang, Q., Luo, G., Ou, J., Yeung, W. S., *J. Chromatogr. A* 1999, *848*, 139-148.

[6] Thormann, W., Wey, A. B., Lurie, I. S., Gerber, H., Byland, C., Malik, N., Hochmeister, M., Gehrig, C., *Electrophoresis* 1999, *20*, 3203-3236.

[7] Henskens, Y., de Winter, J., Pekelharing, M., Ponjee, G., *Clin. Chem.* 1998, *44*, 1184-1190.

[8] Koutny, L. B., Schmalzing, D., Taylor, T. A., Fuchs, M., *Anal. Chem.* 1996, *68*, 18-22.

[9] von Heeren, F., Verpoorte, E., Manz, A., Thormann, W., *Anal. Chem.* 1996, *68*, 2044-2053.

[10] Chiem, N. H., Harrison, D. J., *Clin. Chem.* 1998, *44*, 591-598.

[11] Mangru, S. D., Harrison, D. J., *Electrophoresis* 1998, *19*, 2301-2307.

[12] Schult, K., Katerkamp, A., Trau, D., Grawe, F., Cammann, K., Meusel, M., *Anal Chem* 1999, *71*, 5430-5435.

[13] Sato, K., Tokeshi, M., Odake, T., Kimura, H., Ooi, T., Nakao, M., Kitamori, T., *Anal. Chem.* 2000, *72*, 1144-1147.

[14] Sato, K., Tokeshi, M., Kimura, H., Kitamori, T., *Anal. Chem.* 2001, *73*, 1213-1218.

[15] Yang, T., Jung, S., Mao, H., Cremer, P. S., *Anal. Chem.* 2001, *73*, 165-169.

[16] Eteshola, E., Leckband, D., *Sensors and Actuators B* 2001, *72*, 129-133.

[17] Dodge, A., Fluri, K., Verpoorte, E., de Rooij, N. F., *Anal. Chem.* 2001, *73*, 3400-3409.

[18] Bernard, A., Michel, B., Delamarche, E., *Anal. Chem.* 2001, *73*, 8-12.

[19] Linder, V., Verpoorte, E., Thormann, W., de Rooij, N. F., Sigrist, H., *Anal. Chem.* 2001, *73*, 4181-4189.